ISTANBUL TECHNICAL UNIVERSITY ★ INSTITUTE OF ENERGY

SORTING SINGLE WALL CARBON NANOTUBES BY ELECTRONIC STRUCTURE USING GEL CHROMATOGRAPHY

M.Sc. THESIS

FERESHTEH ORDOKHANI

Energy Science & Technology Division

Energy Science & Technology Programme

Thesis Advisor: Prof. Dr. Nilgün KARATEPE YAVUZ

AUGUST 2016

ISTANBUL TECHNICAL UNIVERSITY ★ INSTITUTE OF ENERGY

SORTING SINGLE WALL CARBON NANOTUBES BY ELECTRONIC STRUCTURE USING GEL CHROMATOGRAPHY

M.Sc. THESIS

FERESHTEH ORDOKHANI
(301131044)

Energy Science & Technology Division

Energy Science & Technology Programme

Thesis Advisor: Prof. Dr. Nilgün KARATEPE YAVUZ

AUGUST 2016

İSTANBUL TEKNİK ÜNİVERSİTESİ ★ ENERJİ ENSTİTÜSÜ

TEK DUVARLI KARBON NANOTÜPLERİN ELEKTRONİK YAPILARINA GÖRE JEL KROMATOGRAFİ YÖNTEMİ İLE AYRILMASI

YÜKSEK LİSANS TEZİ

FERESHTEH ORDOKHANI
(301131044)

Enerji Bilim ve Teknoloji Anabilim Dalı

Enerji Bilimi ve Teknoloji Programı

Tez Danışmanı: Prof. Dr. Nilgün KARATEPE YAVUZ

AĞUSTOS 2016

FERESHTEH ORDOKHANI, a **M.Sc.** student of ITU **Institute of Energy** student ID 301131044, successfully defended the **thesis** entitled "**SORTING SINGLE WALL CARBON NANOTUBES BY ELECTRONIC STRUCTURE USING GEL CHROMATOGRAPHY**", which she prepared after fulfilling the requirements specified in the associated legislations, before the jury whose signatures are below.

Thesis Advisor:	**Prof. Dr. Nilgün KARATEPE YAVUZ** İstanbul Technical University
Jury Members:	**Prof. Dr.** **Yeşim Hepuzer Gürsel** İstanbul Technical University
	Doç. Dr. **Fevzihan Başarır** Tubitak Marmara Research Center

Date of Submission: 2 May 2016
Date of Defense: 5 August 2016

Thank you for your love, support, encouragement and dedication throughout my life.

To my parents and my spouse

FOREWORD

I would like to express my sincere gratitude to my supervisor Prof. Dr. Nilgün KARATEPE YAVUZ for sparing so much of her time, advices and encouragements through the study. Without her guidance and support this work could not have been accomplished.
I would also like to thank Prof.Dr. Yeşim Hepuzer Gürsel and Rüya Atlıbatür for their invaluable support.
Lastly and most importantly, I thank my family, for their love and never ending support of all my decisions.

May 2016   Fereshteh ORDOKHANI

TABLE OF CONTENTS

ABBREVIATIONS

SWCNT   **:** Single wall carbon nanotube
Hipco   **:** High pressure carbon monoxide
SDS   **:** Sodium dodecyl sulfate
SC   **:** Sodium cholate
DOC   **:** Sodium deoxycholate
DI   **:** Deionized
PEG   **:** Polyethylene glycol
NMP   **:** N-methyl-2-pyrrolidone
CTAB   **:** Cetyltrimethylammonium bromide
CSA   **:** Chondroitin sulfate
AGE   **:** Agarose gel electrophoresis
DOS   **:** Density of States
TEM   **:** Transmission electron microscopy
TGA   **:** Thermogravimetric Analysis

LIST OF SYMBOLS

d   **:** Diameter
$\mathbf{E_{gap}}$ **:** Energy gap
I   **:** Current
L   **:** Length

LIST OF FIGURES

SORTING CARBON NANOTUBES BY ELECTRONIC STRUCTURE USING GEL CHROMATOGRAPHY

SUMMARY

Because of their unique and excellent mechanical, electrical and optical properties, many potential applications of single-walled carbon nanotubes (SWCNTs) have been studied extensively. Synthesis methods developed so far are incapable of producing SWCNTs of defined structures at significant scale and therefore, separation of synthetic mixtures of SWCNTs is both scientifically interesting and technologically important. On the basis of their electronic structures, SWCNTs can be classified into two categories: metallic (m-SWCNTs) and semiconducting SWCNTs (s-SWCNTs). In many cases, metallic SWCNTs are separated from semiconducting SWCNTs and enriched in the supernatant due to stronger interaction between metallic SWCNTs and adsorbates. Separated metallic and semiconducting SWCNTs offer many unique opportunities for a variety of technological applications. Regarding metallic SWCNTs, their extremely high electrical conductivity is well-established (estimated theoretically as high as 10^6 S/cm), and the propagation of electrons in metallic nanotubes is known to be ballistic, largely free from scattering over a distance of thousands of atoms. With their resistance approaching the theoretical lower limits, metallic nanotubes may, in principle, carry an electrical current density of 4-10^9 A/cm2, which is more than 1000 times greater than that in metals such as copper. Indeed, since the first fabrication and investigation of electrical devices based on metallic SWCNTs in 1997, subsequently pursued potential applications have included nanocircuitry, conductive polymeric nanocomposites, and, most extensively, transparent conductive coatings/films. Post-synthesis separation of m-SWCNTs and s-SWCNTs remains a challenging process. Consequently, there have been intense efforts to develop various postgrowth techniques for separating SWCNTs, including dielectrophoresis, ultracentrifugation and gel chromatography. Several of methods have been demonstrated to achieve high-purity separation of m- and s-SWCNTs. Gel chromatography is emerging as an efficient and large scale separation technique. In this separation strategy, dispersions of nanotubes in the surfactant sodium dodecyl sulfate (SDS) are passed through a gel matrix which is usually composed of Agarose or cross linked allyl dextran gel beads. In the ideal case, metallic species pass through the gel and are obtained in the initial eluate, while semiconducting species are adsorbed to the stationary phase and may be collected by changing the eluent. The mechanism behind the separation is believed to be related to conformational differences between SDS adsorbed on metallic and semiconducting species, rather than any size exclusion effects due to selective aggregation or dispersion of either nanotube type. A recent study has shown that for hydrogel media, metallic CNT species dispersed in SDS have a higher enthalpy of adsorption than do their semiconducting counterparts, which leads to a difference in the free energy of adsorption.

Consequently, under appropriate conditions the two electronic types may be separated. It has also been shown that the differences in adsorption that allow separation by electronic type extend to allow sorting of semiconducting nanotubes into fractions enriched in individual species, which may be accomplished at a fixed SDS concentration of 1 wt.% by utilising multiple gel columns. However, the full (100%) separation has not been achieved yet, mainly due to the lack of understanding of the underlying mechanism.

In this study, we successfully separated m- and s-SWCNTs using an allyl dextran-based size-exclusion gel (Sephacryl S-200, GE Healthcare). We used this gel as the medium and sodium dodecyl sulphate (SDS) for Hipco SWCNT dispersion. First separation of metallic and semiconducting SWCNTs was done so that we can assure that the greatest amount of s-SWCNTs adsorbed to the column, thus allowing for better separation of the semiconducting species as they adsorb to the gel. Smaller diameter SWCNTs with higher affinity will adsorb more strongly to the column while large diameter SWCNTs will adsorb weakly to the column, thus creating a gradient in the column from smaller diameter SWCNT to larger diameter SWCNTs. 1 % M SDS was able to elute the metallic SWCNTs while leaving the majority of the semiconducting SWCNTs bound to the column. The s-SWCNTs were eluted with 5% M SDS and 1% SC. To achieve the effective separation, we considered SWCNTs adsorbtion to Agarose gel respectively, large diameter s-SWCNTs adsorb more strongly to the column with Agarose gel.

Finally, the separation achieved will be characterized with UV-VIS-NIR, Raman and spectroscopy.

TEK DUVARLI KARBON NANOTÜPLERİN ELEKTRONİK YAPILARINA GÖRE JEL KROMATOGRAFİ YÖNTEMİ İLE AYRILMASI

ÖZET

Nanoteknolojinin gelişmesinde önemli rol oynayan karbon yapılı malzemeler, yapısal çeşitliliği ve işlenebilirliği ile bilim dünyasının oldukça üzerinde durduğu araştırma konuları arasındadır. Nanoölçekteki çalışmalarda atomik seviyeden kaynaklanan yapısal farklılıklar elde edilen malzemenin işlenebilirliğini büyük ölçüde etkilemektedir. Karbon nanotüplerin keşfedilmesi nanoteknoloji uygulamalarında bir devrim niteliği taşırken üstün mekanik, termal, elektriksel ve optik özelliklere sahip atomik ve moleküler yapıları sebebi ile bilim dünyasının başlıca araştırma konuları arasında yerini almıştır. Bu noktada, bilimsel araştırmaların endüstriyel alanlara taşınması süreçleri karbon nanotüplerin üretim yöntemlerine bağlı olarak türlerine ve özelliklerine göre değişim göstermektedir. Karbon nanotüp üzerine yapılan çalışmaların ilerleyişi ise kullanım alanlarının çeşitliliği ile paralellik göstermektedir. Nanotüplerin sentez koşullarının belirli parametreler yardımıyla iyileştirilmesi ile kullanım alanı genişlemiş olup yaygın uygulamaları biyosensörler, hidrojen depolama üniteleri, kompozit malzemeler ve kapasitörler şeklinde örneklendirilebilir.

Tek duvarlı karbon nanotüpler (TDKNT'ler), Iijima'nın 1993 yılında keşfinden bu yana, üstün mekanik, termal, elektriksel ve optik özelliklerinden dolayı önemli ölçüde ilgi çekmektedir. Çaplarına ve kiralitelerine bağlı olarak üçte bir metalik ve üçte iki yarı iletken karakter taşıdığı bilinen TDKNT'lerin elektronik cihaz uygulamalarında daha yüksek verim ile ayrılması TDKNT'ler için büyük bir önem taşımaktadır. Ancak, bu zamana kadar TDKNT'lerin istenilen yapıda ve endüstriyel ölçekte üretimi için belirli bir proses geliştirilememiş, böylelikle TDKNT'lerin elektronik yapılarına göre ayrılması bilim dünyasında oldukça önem kazanmıştır. Bu yapılar metalik ve yarı iletken şeklinde sınıflandırılmakla birlikte genellikle metalik TDKNT'lerin adsorbantlar ile daha güçlü etkileşmesi sonucu yarı iletken TDKNT'lerden ayrılması işlemleri uygulanmaktadır. Yapısal özelliklerine bağlı olarak metalik ve yarı iletken nanotüpler çeşitli alanlarda kullanılmaktadır; örneğin, metalik nanotüpler, daha yüksek verim elde etmek amacıyla transparan iletken filmler ve nanometre boyutlu kondüktörlerde yer almaktadır. Son yıllarda ise, yarı iletken TDKNT'lerin doplama ve yüksek elektron mobilite özelliklerinden dolayı elektronik cihaz uygulamalarında etkinliğin arttırılması amacıyla çeşitli çalışmalar yapılmaktadır.

Karbon nanotüplerin üretiminde farklı tekniklerin geliştirilmesinin yanı sıra en çok kullanılan yöntemler; katı halde karbondan sentezlenen ark boşalım ve lazerle aşındırma ile gaz halde karbondan sentezlenen kimyasal buhar birikimidir. Nanotüplerin miktarı uygulama alanına bağlı olarak değişim göstermekle birlikte kullanılan karbon kaynağı, sıcaklık, basınç ve katalizör gibi çeşitli parametreler üretim prosesinin sürekliliği ve kapasitesi açısından büyük önem taşımaktadır. Bu etmenler göz önünde bulundurulduğunda kimyasal buhar birikimi yöntemi diğer yöntemlere göre daha düşük maliyetli olması ve endüstriyel ölçekteki üretimi mümkün kılması nedeniyle sıklıkla kullanılmaktadır. Kimyasal buhar birikim yönteminin dahilinde lazer destekli, mikrodalga destekli, termal destekli modellemeleri geliştirilmiştir. Bu

yöntemin farklı bir türü olan HiPco (yüksek basınçlı karbon monoksit) ise geniş çapta üretimi mümkün kılması sebebiyle literatürde çokça çalışmaya konu olmaktadır.

Literatürde TDKNT'lerin seçici üretimi için çeşitli ileri teknikler uygulanmasına rağmen ayırmaya yönelik belirli bir metodoloji henüz geliştirilememiştir. Ancak, etkin bir ayrımın gerçekleştirilebilmesi açısından uygun çözücü ortamında nanotüplerin kristal yapısına zarar vermeyecek şekilde dispers edilmesi oldukça önem taşımaktadır. Çünkü TDKNT'ler yığın halinde üretilmekle birlikte su ya da çoğu organik çözücü varlığında aglomere olmakta, iyi bir dağılım gösterememektedir. Literatürde, iyonik yüzey aktif maddelerin kullanımıyla bu sorun giderilmiş ve geliştirilen suda çözülebilir sentetik polimer, protein ve dispersantlar ile nanotüplerin dağılımının yanı sıra kovalent olmayan fonksiyonlaştırma işlemleriyle bu bileşiklerin seçici ayrım özelliği kazanması sağlanmıştır.

Elektronik yapılarına göre ayrımı gerçekleştirilen TDKNT'ler genellikle laboratuvar ölçekli elde edilmekle beraber endüstriyel çapta üretimi ilk defa kromatografi yöntemiyle sağlanmıştır. Bu yöntem, ucuz, basit ve çevreye zarar veren kimyasal maddeler içermemesi sebebiyle son zamanlarda oldukça çalışmaya konu olmaktadır. Ancak, literatürde TDKNT'lerin çeşitli yöntemler ile ayrılmasında pek çok işlem uygulanmasına rağmen istenilen kiralite ve çapta nanotüp eldesine yönelik belirli bir sistem geliştirilememiştir.

Bu tez çalışmasında, kimyasal yöntemlerden biri olan jel kromatografi yöntemi kullanılarak nanotüplerin jel ve yüzey aktif madde ile moleküler etkileşimi incelenmiştir. Jel kromatografi yöntemi ile TDKNT'lerin elektronik özelliklerine göre ayrılması işlemleri, anyonik yüzey aktif madde varlığında dispersiyonun gerçekleştirilmesinin ardından kolon yardımıyla sabit faz olarak kullanılan sefakril 200 jel ortamında, hareketli fazı ikili sistemin oluşturduğu anyonik yüzey aktif maddeler ile farklı derişimlerde hazırlanarak gerçekleştirilmiştir. Ayrıca literatürden farklı olarak iki ayrı jelin sabit faz olarak kullanıldığı çalışmada, yalnızca dört kolon ile yarı iletken TDKNT'lerin yüksek verimle ayrılması sağlanmıştır. Çaplarına ve kiralitelerine gore değişim gösteren nanotüp-sabit faz ve nanotüp-hareketli faz etkileşimleri sonucunda sefakril 200 jel ortamında kolondan elde edilen yarı iletken TDKNT'ler mavi renkte, agaroz jel ortamında elde edilen yarı iletken TDKNT'ler ise yeşil renkte gözlenmiştir. Metalik TDKNT'ler ise her iki sabit faz ortamında kahverengi olarak gözlenmiştir. Bu çalışmaların yanı sıra ayrımı sağlanan TDKNT'lerin yarı iletken ve metalik yapılarını zenginleştirmek amacıyla kolondan alınan, metalik içeriği fazla olarak fraksiyonlanan çözelti tekrar kolondan geçirilmiş ve böylece yarı iletken ve metalik içeriği zengin TDKNT'ler elde edilmiştir.

Metalik ve yarı iletken özelliklerine göre ayrımı sağlanan TDKNT'ler, UV-vis-NIR ve Raman spektroskopi yöntemleri kullanılarak karakterize edilmiştir. Optik absorpsiyon spektroskopisi yöntemiyle metalik ve yarı iletken TDKNT'lerin analizi 400-1350 nm dalga boyları arasında yapılmıştır. Metalikçe zengin TDKNT'lerin birinci geçiş enerjisi 450-660 nm (M11) dalga boyunda, yarı iletkence zengin TDKNT'lerin birinci geçiş enerjisi 850-1350 nm (S11) dalga boyunda ve ikinci geçiş enerjisi 630-900 nm (S22) dalga boyunda absorpsiyon pikleri gözlenmiştir. Piklerin yüzey aktif madde derişimine bağlı olarak çeşitli bölgelerde ve farklı şiddetlerde gözlenmesi, nanotüplerin çözelti içerisinde çap ve kiraliteye bağlı olarak değişim göstermesinden kaynaklanmaktadır.

Raman spektrumları incelendiğinde; nanotüpe özgü olan radyal soluklanma modu (RBM) bandı piki 100-500 cm^{-1} aralığında, sivri ve şiddetli G bandı piki 1550-1595 cm^{-1} aralığında ve yapıdaki kusurları gösteren D bandı piki 1250-1450 cm^{-1} aralığında oldukça zayıf ve küçük şekilde gözlenmiştir. Literatürde, G⁻ bandının genişliğinin

metalik TDKNT'ler için karakteristik özellik göstermesine rağmen, burada meydana gelen piklerin koltuk tipi (n=m) TDKNT'leri içermediği ve koltuk tipi nanotüplerin G^+ bandının bulunduğu bölgede dar ve tek bir pik olarak gözlendiği tespit edilmiştir. Böylelikle, sadece G^- bandı bölgesi kullanılarak karışım halindeki TDKNT'lerin elektronik yapı analizi mümkün olmamaktadır. Elde edilen sonuçların diğer yöntemler ile desteklenmesi büyük önem taşımaktadır. Ancak, D bandında bulunan piklerin varlığı nanotüplerin kristal yapısının değerlendirilmesi açısından önemli olup bu çalışmada D bandında bulunan piklerin düşük şiddette gözlenmesi ayırma işlemleri sonucunda yapıda önemli ölçüde bir hasar meydana gelmediğinin göstergesidir.

Kalitatif analizin temel alındığı çalışmada, ayırma verimi, ticari olarak kullanılan malzemenin analiz sonuçları karşılaştırılarak değerlendirilmiştir. Yapılan çalışmada ticari TDKNT ile karşılaştırıldığında, (çaptan kaynaklanan) farklı kiralitede ve yarı iletkence zengin TDKNT nanotüplerin elde edildiği gözlemlenmiştir.

1. INTRODUCTION

In the last decade due demand of last generation of high technology materials, there is a tremendous interest in nanotechnology [1]. Due to their marvellous material properties nanomaterials differ from the isolated atom and the bulk phase.

Nanotechnology aims to production and improvement of smaller, cheaper, lighter, faster device with more functionality and less raw material and energy. Therefore, nanotechnology deals with materials having a size of 1100 nanometer (nm). The properties of the material changes as the size of the material decreases. When the nanomaterials are considered, surface behaviour of the material dominates the behaviour of the overall material. Nanomaterials their mechanical, electrical, and optical properties improve. Therefore, they can be implicated to many fields such as electronics, chemicals, sensors, and biotechnology.

The identification of the structure of fullerenes in 1985 by Kroto and his friends was a breakthrough in nanotechnology [2]. It was followed by the discovery of multi walled carbon nanotubes (MWCNTs) in 1991 and single wall carbon nanotubes (SWCNTs) in 1993 by lijima [3, 4].

The unique one-dimensional (1-D) quantum confined properties of carbon nanotubes (SWCNTs) have sparked considerable interest in the scientific and technological community [5,6]. As-prepared SWCNTs, however, naturally contain two different species of tubes namely the semiconducting SWCNT (S-SWCNT) and metallic SWCNT (M-SWCNT). Different species of carbon nanotubes are used for different applications, SWCNTs have the potential to revolutionize numerous applications where nanosized metallic and/or semiconducting components are required along with high strength [7,8] large flexibility [9] and superb chemical stability [10,11]. In particular, metallic SWCNTs are highly suited for nanoscale circuits, [12] ultrathin, flexible and transparent conductors, [13] supercapacitors, [14] field emitters, [15] Actuators, [16] and nanosized electrochemical probes [17]. Semiconducting SWCNTs on the other hand, are applicable for nanoscale sensors, [18] transistors, [19] and photovoltaic devices [20].

Statistically, one-third of these structures are metallic and the other two-thirds are semiconducting. It is therefore imperative to separate the two species of nanotubes before integrating it in electronics. Several methods are described in the literature to sort semiconducting from metallic SWCNTs , including dielectrophoresis, [21] DNA-assisted separation, [22]   selective polymer wrapping, [23], Gel Agarose chromatography [24-26] , Density Gradient Ultracentrifugation (DGU) [27] and amine extraction [28].

Post-synthesis separation of metallic (m-SWCNTs) and semiconducting (s-SWCNTs) single-wall carbon nanotubes (SWCNTs) remains a challenging process. Gel Agarose chromatography is emerging as an efficient and large scale separation technique. However, the full (100%) separation has not been achieved yet, mainly due to the lack of understanding of the underlying mechanism. Here, we study the PH effect on the SWCNTs separation via gel Agarose chromatography. Exploiting a gel Agarose micro-beads filtration technique, was achieved up to 70% m-SWCNTs and over 90% s-SWCNTs. Chromatography allows for separation of metallic from semiconducting through the use of a stationary phase such as Sephacryl-200 or Agarose gels and a mobile phase of 1 wt% SDS. the interaction between nanotubes and the gel is expected to be similar to that in the SDS system, where s-SWCNTs have higher affinity towards the gel compared with m-SWCNTs. Consequently, during the elution, s-SWCNTs adsorb onto the gel to a much greater extent, which results in a longer time to flow through the gel than m-SWCNTs. Metallic nanotubes elute from the column and result in a brown fraction, while semiconducting SWCNTs elute second and result in a purple-blue-green fraction. The dominant mechanism affording this electronic SWCNT type separation is still a significant research area.

For gel chromatography, either ally dextran or Agarose gel are mostly used in previously reported literature. Novelty of this research relies on using both of these gels for increasing the efficiency of the separation. According to optical absorbance spectra of separated s-SWCNT, small s-SWCNTs are adsorbed to dextran gel beads whereas large s-SWCNTs are adsorbed to Agarose gel beads. Considering these properties, our group have developed a novel mixed method for separation of m-SWCNTs and s-SWCNTs by using dextran and Agarose gels respectively. By applying a SWCNTs/SDS dispersion to a column containing dextran, small s-SWCNTs observed to be adsorbed to the gel and collected by changing the eluent. This process was repeated for obtained unbundle solution until there was no any

absorption to the gel. Subsequently, the operation continues with Agarose gel beads for absorbing the large s-SWCNTs repeatedly until the end of adsorption process. In the end, we separated nearly all of the small and large s-SWCNTs and m-SWCNTs that passed through the final column as unbundle solution.

This method while being low-cost, can be done in large-scale with very high efficiency (without missing large amount of initial raw SWCNTs).

Chapter 2 of this thesis will be about SWCNTs structure and properties, In Chapter 3 will been discussed about SWCNTs separation methods and Chapter 4 will be about SWCNT characterization methods.

Chapter 5 presents the experimental studies performed at this work. It includes SWCNTs separation processes and characterization of separated SWCNTs as metallic and semiconducting.

Chapter 6 offers the results of SWCNTs separation and characterization. It includes evaluation spectroscopy piks of separated SWCNTs in this study with the over 90% purified s and m-SWCNTs that exist in literature.

The overall results and recommendations for this study are given in Chapter 7.

2. CARBON NANOTUBES

2.1 Carbon Allotropes

Carbon is the basic constituent of all organic matter and the key element of the compounds that form the huge and very complex discipline of organic chemistry. Carbon is different from other elements in one important respect, that is its diversity which can be attributed to the ability to form different bonds [29]. Carbon can have different and important properties depending on its bonding structure and possible atomic configuration. Each carbon atom has six electrons, occupying $1s^2$, $2s^2$, $2p^2$ orbitals. Electrons occupying $2s^2$ and $2p^2$ orbitals are valence electrons which can form different covalent bonds depending on the hybridization type. Common carbon allotropes such as diamond, graphite, nanotubes of fullerenes have different bonding structure due to different hybrid orbitals as shown in Figure 2.1.

sp^3 hybrid structure, demonstrated in Figure 2.1 (a), has a tetrahedral geometry and composed of three p orbitals and one s orbital, forming strong covalent sigma (σ) bonds. sp^2 hybridized atoms shown in Figure 2.1 (b) have trigonal geometries combining the s orbital with two p orbitals and forming σ bonds, while other two p orbitals are forming pi (π) bonds. sp hybrid structure is a combination of one s and one p orbital which has a linear geometry as shown in Figure 2.1 (c).
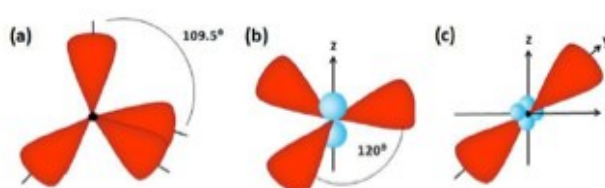
Figure 2.1 : (a) sp^3, (b) sp^2, (c) sp hybridized carbon atoms.

Diamond has a tetrahedral crystal structure and each sp^3 hybridized carbon atom is bonded to four other atoms with σ bonds, as shown in Figure 2.2 (a). Diamond is the hardest (Mohs hardness 10), naturally occurred material because of this firmly constructed arrangement. Diamond is a wide gap semiconductor (5.47 eV) and has

the highest thermal conductivity ($\sim$25 $Wcm^{-1}K^{-1}$) and the highest melting point (4500 K).

Graphite is another carbon allotrope, which consists of the sp^2 hybridized atoms. In each carbon atom, three of the four outer shell electrons are hybridized to sp^2 orbitals and form strong covalent σ bonds with the three neighbouring carbon atoms [30]. The remaining valence electron in the π orbital provides the electron band network that is largely responsible for the charge transport in graphene [31]. This bonding structure forms a planar hexagonal network like a honeycomb as shown in Figure 2.2 (b). Monolayer is called a graphene sheet and layers are held together by van der Waals forces. The spacing between two graphene layers is 0.34 nm. Graphite conducts both electricity and heat due to its π bond electrons, which are free to move. Owing to its weak π bonds and the van der Waals interaction between the layers, graphite is a perfect lubricant hence the graphene sheets are able to glide away [32].

A spherical fullerene molecule, C60, is demonstrated in Figure 2.2 (c). C60 molecules are icosahedrals, composed of 20 hexagons and 12 pentagons forming a stable football like structure. Fullerenes are not planar, they have curvatures with some sp^3 character present in the essentially sp^2 hybridized carbons [33]. They have novel properties and so far utilized in electronic, magnetic, optical, chemical, biological and medical applications.
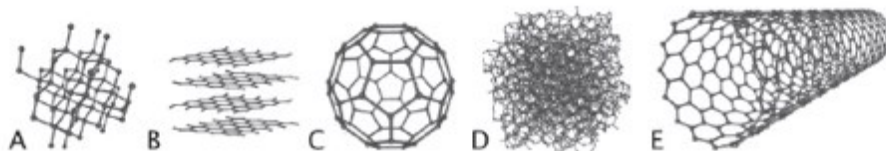
Figure 2.2 : Different allotropes of carbon (a) diamond (b) graphite (c) C60 fullerene (d) amorphous carbon (e) single-walled carbon nanotube.

CNTs are cylindrical nanostructures and formed by rolling of the graphene sheets. They can be open ended or their ends may be capped with bisected of fullerene as shown in Figure 2.2 (d). The sp^2 hybridization, which is the characteristic bonding of graphite, has a significant effect on the formation of the CNTs. Bonding in CNTs fundamentally depends on the sp^2 hybridization, which makes them stable; whereas, the hallow cylindrical part is more strong than the ends of the CNTs due to the presence of sp^3 bonding in the end caps [34].

2.2 Geometric construction of SWCNTs

SWCNTs vary in the diameter of the tube, ranging from 0.7 – 5.0 nm, but are commonly grown with diameters < 2 nm [35-37]. Diameter is one of the two attributes that result in the variation on physical and electrical properties, the other being chirality. When rolling the graphene sheet, the two edges of the graphene sheet have the ability to meet at a variety of different angles, sometimes resulting in chirality of the tube. This chirality of the SWCNT along with its diameter changes overlapping of the sp^2 hybridized carbons resulting in different electrical properties of SWCNTs [38].

When considering a graphene sheet, SWCNTs can be characterized through vector components that will result in the rolling of different SWCNTs, these vectors give insight into the small differences in the diameter and chiral angle of the SWCNT. When considering a unit cell in a graphene sheet, the vectors from the center of the unit cell to the centers of the two adjacent cells can be considered R1 and R2. When rolling a SWCNT from a graphene sheet, the sum of the number horizontal steps (n) and the number of vertical steps (m) results in the roll-up vector of the SWCNT (Equation 2.1).

$$R = n_1 R_1 + m_2 R_2 \qquad (2.1)$$

(n, m) vectors represent the difference in the conformation of the benzene rings in SWCNTs, "n" representing a zigzag conformation of the benzene rings while "m" representing the armchair configuration (Figure 2.1). From the (n, m) values, the diameter and chiral angle of the SWCNT can be calculated from equations 2.2 and 2.3 [39]. For instance, if we consider a SWCNT with an (n, m) of (9,4), then the chiral angle would be $\theta = 17.5°$, and the diameter would be d = 0.916 nm (Fig. 2.1).

$$\cos \theta = \frac{n + \frac{m}{2}}{\sqrt{n^2 + nm + m^2}} \qquad (2.2)$$

$$d = \frac{a}{\pi} \sqrt{n^2 + nm + m^2} \qquad (2.3)$$
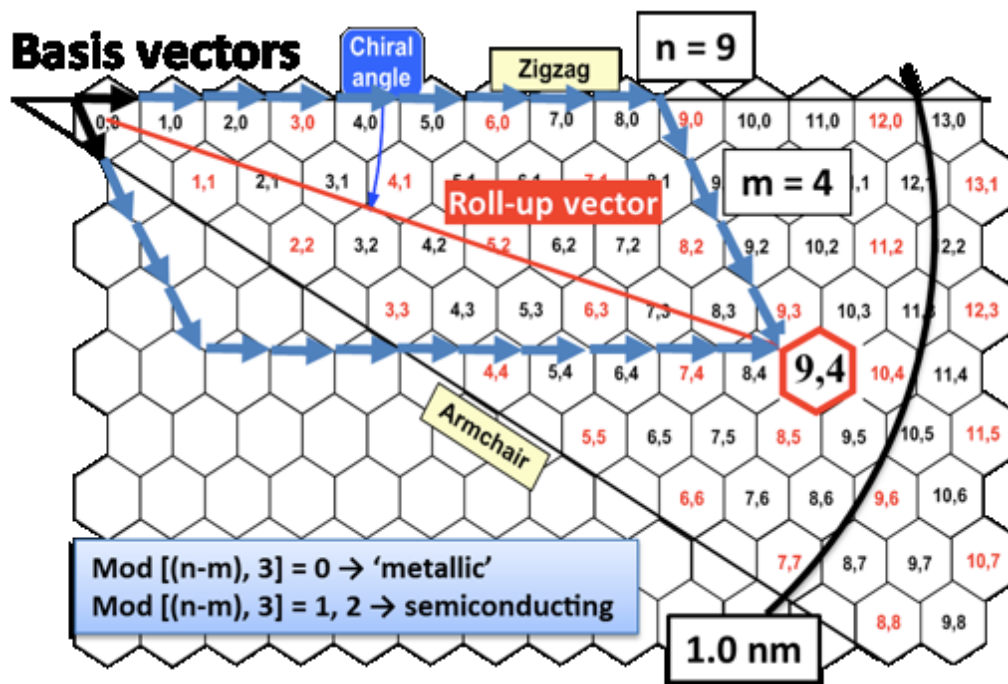
Figure 2.3 : A graphene sheet map, shows the different species of SWCNTs that result for a combination of the n and m values. (n,0) results in a zig-zag SWCNT that has a chiral angle of 0°, (n = m) results in an armchair SWCNT with a chiral angle of 30°. Two thirds of all SWCNTs are semiconducting, while only one third are metallic [42].

In any given sample of single-walled carbon nanotubes there are a variety nanotube with different electrical properties [40]. SWCNTs fall into two different groups of electrical properties, nanotubes that have metallic electrical properties and nanotubes that have semiconducting electrical properties [41]. A general sample set of SWCNTs has a composition of 1/3 metallic SWCNTs and 2/3 semiconducting SWCNTs, indicated by the red and black hexagons, respectively, in Figure 2.1 [42] To determine the electric nature of a single carbon nanotube one can look at the (n, m) of each nanotube, if mod[(n-m),3] = 0 the SWCNT is metallic and mod[(n-m),3] ≠ 0 the SWCNT is semiconducting. This rule allows for trends to be observed in the electronic properties, when n = m the SWCNT is always in the armchair conformation and metallic in the electrical properties, when (n,0) the SWCNT is always in the zig-zag conformation but not always semiconducting. For example, when examining the (7,1) – mod [(7-1),3] = 0, the SWCNT is metallic; while when examining (6,5) – mod[(6-5),3] = 1, the SWCNT is semiconducting. Large-scale production methods have yet to achieve the ability to specifically control the range of species of SWCNTs produced to a single type of either electronic character or (n, m)- species.

2.3 Carbon Nanotube Band Structure

Depending on their structure, carbon nanotubes behave as metallic or semiconducting. Tight Binding calculations [42] show that the nanotubes for which n-m is evenly divisible by 3 have no bandgap (their valence and conduction bands intersect at one point), so they are considered metallic. Other carbon nanotubes have a 1 - 2 eV gap between their valence and conduction bands and therefore are semiconducting (Figure 2.2). Statistically it is predicted that 1/3 of the total number of carbon nanotubes are metallic. For example, all armchair single-walled carbon nanotubes are metallic due to the fact that their n-m value is equal to zero.
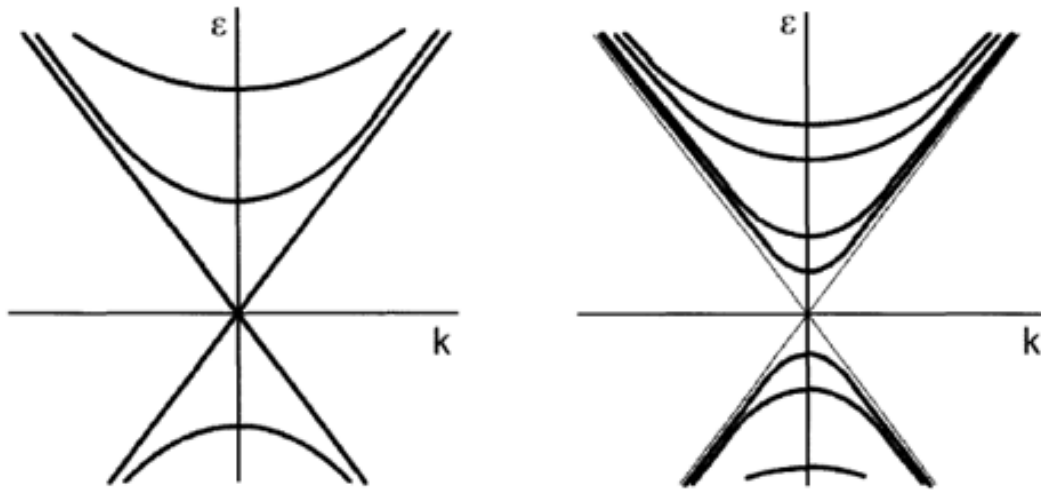
Figure 2.4 : Band structures of metallic (left) and semiconducting (right) singlewalled carbon nanotubes [42].

Due to their 1-dimensional structure, both metallic and semiconducting carbon nanotubes exhibit sharp peaks in their density of electronic states called van Hove singularities. The density of states between c_1 and v_1 sub bands for metallic carbon nanotubes is nonzero (Fig 2.3. a), which also indicates that they have no band gap.

As for semiconducting nanotubes, the band gap is represented by the separation between the first valence (v_1) and first conduction (c_1) sub bands (Fig 2.3. b). Band gap energies En scale approximately inversely with carbon nanotube diameter.

Metallic SWNT

$v_1 \rightarrow c_1$ corresponds to the "first van Hove" optical transition

Semiconducting SWNT

$v_2 \rightarrow c_2$ corresponds to the "second van Hove" optical transition
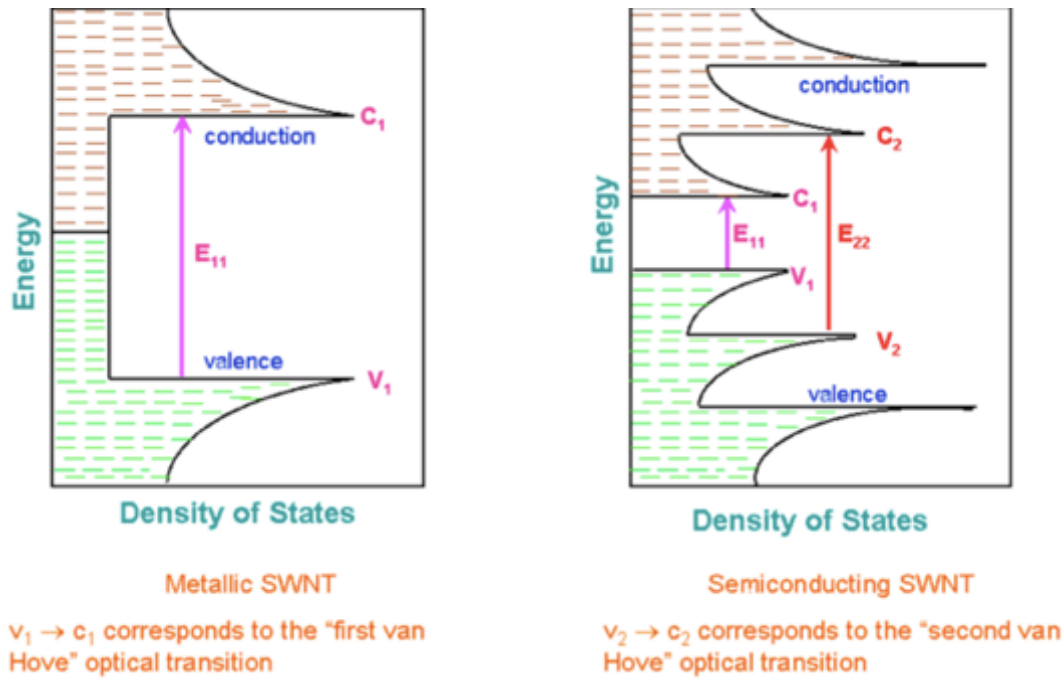
Figure 2.5 : density of states schematic of metallic and semiconducting carbon nanotube [43].

2.4 Properties of SWCNTs

2.4.1 Electronic properties

Depending on the chirality, nanotubes can be either metal or semiconductor even though they have the same diameter [44]. When a graphite sheet is rolled to form CNT not only the carbon atoms are ordered around the circular structure but also quantum mechanical wave functions of the electrons are ordered accordingly. The electrons are bounded in radial directions by the single layered graphite sheet. There exist periodical boundary conditions around the circle of the nanotube. If there are ten hexagons around nanotube then the eleventh hexagon fits to first hexagon. As a result of the quantum boundaries the electrons are effective only along the nanotube axis enabling to determine the wave vectors. Thus small diameter nanotubes are either metallic or semiconductors. According to electrical properties nanotubes can be classified as large gap, tiny gap and zero gap nanotubes. Theoretical calculations show that electrical properties of nanotubes depend on geometric structure. Graphene is a zero gap semiconductor, according to the theory carbon nanotubes can be metals or semiconductors having different energy gaps depending on diameter and helicity of nanotubes. As the nanotube radius R increases the band gap of large gap and tiny gap nanotubes decrease with $1/R$ and $1/R_2$ dependence, respectively [45-47]. The electrical

10

properties of SWCNTs depend on n and m values: If n=m forming armchair nanotube is metallic, if nm= 3k; k € Z, k≠0 the nanotube it is tiny gap semiconductor that is metallic at room temperature If nm= 3k ± 1; k € Z, k≠0 large gap semiconductors. Experimental studies performed by applying electrical field to nanotubes are proving the theoretical calculations. In experimental studies it was observed SWCNT with a diameter of 0.4 nm became conductive at 20 K. In further experimental studies of electronic properties of nanotubes, it was observed that electrical conductivity is dependent on temperature in the range of 2300K [48]. In the measurements of SWCNTs, it was observed that each nanotube acts individual conductivity and the resistivity is at 300 K is in the range of $\sim 1.2 \times 10^{-4}$–5.1×10^{-6}. SWCNT bundles have metallic behaviour with a resistivity of 0.34×10^{-4} to 1.0×10^{-4} whereas copper has a resistivity of 1.7×10^{-6} ohm. Thus we the electrical resistivity of CNTs is very close to copper. Metallic nanotubes have remarkable conductivities. Although a CNT bundle can transport a current density of 1×10^9 A/cm^2 copper wires can transport 1×10^6 A/cm^2 which is thousand times less than CNTs [49].

2.4.2 Mechanical properties

Theoretical calculations demonstrate that the mechanical properties of SWCNTs are also dependent on the dimensions of SWCNTs. The carbon-carbon bond in graphite is one of the strongest, therefore SWCNTs possess the potential of being the strongest material in nature. Theoretical calculations predict that SWCNTs could have a Young's modulus as high as 1-5 TPa. However, it is also predicted that softening may occur with increasing diameter [50]. The tensile strength of SWCNTs is found to be 13-52 GPa and the tensile modulus of SWCNTs ranges from 0.32-1.47 TPa. For comparison, high tensile steel has a tensile strength of 1.6-1.9 GPa, and silicon carbide has a strength of 3 GPa; both are among the strongest materials. The mechanical properties of SWCNTs have made them useful in many important applications. For example, the desired tensile strength for a space elevator is about 62 GPa [50]. Thus, SWCNTs can be promising candidates for this application. Observations in a transmission electron microscope (TEM) show that SWCNTs are very resistant to breaking when bent [51, 52]. This flexibility is related to the ability of carbon atoms in the planar graphene sheet to rehybridize [51]. Such flexibility is also very important in nanoprobe tips to endure stress [51].

2.4.3 Optical properties

Many of the unique optical properties of SWCNTs arise from quantum size effects. The SWCNT diameter is smaller than the Bohr exciton radius, so electrons and holes are confined spatially and discrete electronic energy levels are formed [51]. The energy separation between adjacent levels increases with decreasing dimensions, similar to a particle in a box [51]. Therefore, the electronic configuration is significantly different from the bulk material. When photons strike SWCNTs, the ground state electrons can absorb the photon energy and move into excited states. In the visible-near infrared spectral range, the absorption spectra of SWCNTs show three sets of absorption bands,

corresponding to the first (S_{11}) and second (S_{22}) allowed transitions for semiconducting nanotubes and the first (M_{11}) allowed transition for metallic nanotubes [53]. The first inter band transition (S_{11}), in which valence band electrons move to the conduction band, has an energy in the near infrared. Therefore, SWCNTs have distinguished absorption features in the near infrared region [54,55]. When the excited electrons fall back to the ground state, emission occurs. Larger diameternanotubes have smaller inter band transition energies (band gaps) as shown in below Equations [56].

$$E_s{}^{11} = 2aC - C\gamma 0/dt \qquad (2.4)$$

$$E_s{}^{22} = 4aC - C\gamma 0/dt \qquad (2.5)$$

$$E_m{}^{11} = 6aC - C\gamma 0/dt \qquad (2.6)$$

Isolation of individual SWCNTs is critical for elucidating the fine structure in the spectrum that can be obscured by strong intertube coupling and inhomogeneity in the nanotube structures [53]. The absorption features can provide rich information about the electronic interband transitions [57]. Based on the UV-Vis-NIR spectral analysis, it has been found that band gaps of SWCNTs can be tuned by chemical modifications or a doping/dedoping process. In particular, the S_{11} optical transitions of semiconducting nanotubes are sensitive to the surrounding environment, which makes them suitable for nanoscale optical sensors [54, 55].

Raman spectroscopy is often used to characterize the SWCNT diameter and Helicity [51,57]. The DOS, which indicates the number of energy states per energy difference, is unique to SWCNTs of a specific helicity [57]. An intense Raman signal is detected as a result of the strong coupling between the electrons and phonons of the nanotube under resonance condition, when the photon energy matches that of the inter band transition [57]. The lower energy Radial Breathing Mode (RBM) reveals the diameter and chirality of SWCNTs. The tangential C-C Stretch G-band can be used to distinguish semiconducting and metallic SWCNTs [58].

In addition to the above mentioned properties, SWCNTs also possess very useful thermal properties. The thermal conductivity of SWCNTs is extremely high and is even better than that of diamond.

2.4.4 Thermal properties

As well as their electrical and mechanical properties CNTs have a reputation for their thermal properties. Nanomaterials are affected by quantum properties. Low temperature, specific heat and the interaction CNTs with each other are considered to count phonons of CNT. Thermal properties of CNTs have been both theoretically and experimentally investigated. Theoretically thermal conductivity of CNTs is better than graphite. In research, thermal conductivity of SWCNTs was measured to be 200W/mK whereas MWCNTs had an electrical conductivity of 300W/mK [59]. As result of Fermi level current density, metallic SWCNT is a one dimensional metal. It has a linear electronic thermal capacity at low temperatures. Theoretically MWCNTs are expected to have lower thermal conductivity than graphite which has low thermal conductivity due to weak Van der Waals forces. MWCNTs have only Van der Waals forces between the nanotube layers. Thermal expansion of CNTs is expected to be better than graphite. It was a matter of question whether CNTs would have high thermal conductivity due to high thermal conductivities of diamond and graphite. The thermal conductivity is the ability of material to transport the heat from high temperature region to low temperature region as shown in Formula 2.7 where q is the change of heat in unit time per unit area, k is the thermal conductivity coefficient, and dT/dx is the thermal gradient along the material.

$$\dot{q}^{"} = -k\frac{dT}{dX} \qquad\qquad (2.7)$$

Thermal conductivity of diamond is 1000-2600 W/mK and graphite is 120 W/mK at 100°C. Hone et al. calculated the thermal conductivity of an individual SWCNT as 1800-6000 W/mK at room temperature [60]. However, researches, it was found to be 2980 W/mK and 6600 W/mK at room temperature [61,62]. Thermal conductivity of MWCNTs are in the range of 1800 to 6000 W/mK.

2.4.5 Chemical properties

Due to their small radius, large specific surfaces and hybridisation CNTs have strong sensitivity to chemical interactions. As a result of this fact they are attractive materials for chemical and biological applications. However, these properties challenge the characterisation of CNTs and determination their properties.

Reactivity of CNTs are determined by direction of π orbitals and pyramidisation of the chemical bonds. Some bond in CNTs are neither perpendicular nor parallel to the tube axis. Therefore, π orbitals cannot be properly directed which affects the reactivity of the CNT. As the diameter of CNT decreases the reactivity of CNT increases.

As a result of the chemical stability and perfect structure of the CNTs the carrier mobility at high gate fields may not be affected by processing like in the conventional semiconductor channels. Nonetheless, low scattering, with the strong chemical bonding and extraordinary thermal conductivity, allows CNTs to withstand extremely high current densities up to $\sim 109 A/ cm^2$ [63].

2.5 Synthesis Methods of Carbon Nanotubes

As CNTs have wide range of applications, the growth techniques which can sustain high purity, and more amount of CNT becomes crucial. CNT synthesis can be achieved by different methods such as:

- Arc discharge

- Laser ablation

- Chemical vapor deposition (CVD)

2.5.1 Arc discharge

In 1991 Lijima reported formation of carbon nanotubes with arc discharge method which is previously used for production of fullerenes [3]. The tubes were produced with diameters ranging from 4 to30 nm and having lengths up to 1μm [64]. In arc discharge method as shown in Figure 2.4 a direct current electric arc discharge in inert gas atmosphere is produced by using two graphite electrodes [4, 64, 65]. The carbon nanotubes grow on the negative end of the carbon electrode that is producing the direct current while Argon as inert gas passes through the system. In arc discharge method a power supply of low voltage (12 to 25 V) and high current (50 to 120 A) is used. Catalyst, Ar: He gas ratio, the distance between the anode and the cathode, the overall gas pressure are the other parameters affecting the quality and the properties (i.e. diameter, yield percent) of CNT synthesized by arc discharge method.
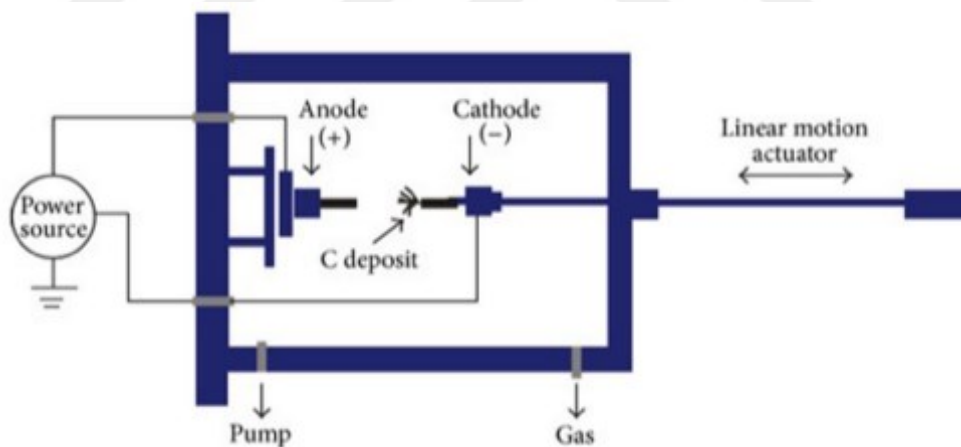
Figure 2.6 : Diagram of arc discharge method.

In an arc discharge process CNTs are prepared with a power supply of low voltage and high current. While the positive electrode is consumed in the arc discharge gas atmosphere (i.e. Ar, He) CNT bundles are formed on the negative electrode [66]. Length of MWCNTs produced by arc discharge method are generally around 1μm having a length to diameter ratio (aspect ratio) of 100 to 1000 [67]. As a result of high aspect ratio and small diameter of the produced MWCNTs they are classified as 1D carbon systems. It has been reported that in the production of SWCNTs by arc

discharge method existence of catalyst (i.e. Fe, Co etc.) is required. Many catalyst compositions can produce MWCNTs but it is observed that Y:Ni mixture yield up to 90% with an average diameter of 1.2 to 1.4 nm [68].

2.5.2 Laser ablation

Laser ablation method is very similar to arc discharge method as it also uses a metal impregnated carbon source to produce SWCNT and MWNT [69]. The laser ablation method Co:Ni atomic percent of 1.2% and 98.8% of graphite composite in an inert atmosphere around 500 Torr of He or Ar in a quartz tube furnace of 1200ºC [38]. Treated to laser light as pulsed or continuously, the nano sized metal particles formed in the vaporized graphite; catalyse the growth of SWCNT and by products. These products are condensed on the cold finger downstream of the source as shown in Figure 2.5 [70]. Smiley group in Rice University achieved the first large scale production of SWCNTs by laser ablation method in 1996 [67]. The production yield of weight varies between 20 to 80% SWCNTs. The diameters of produced SWCNTs are between 1.0 to 1.6 nm.
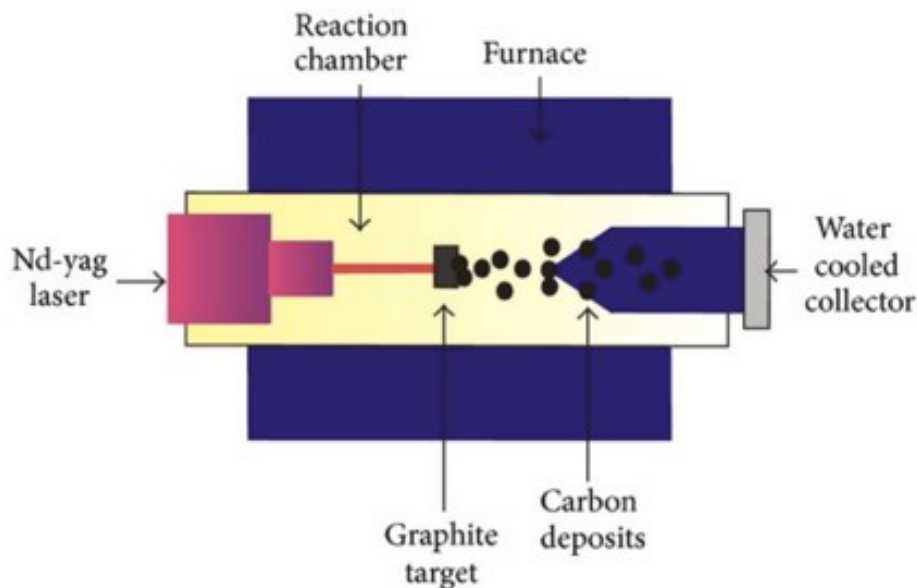
Figure 2.7 : Schematic view of laser ablation furnace.

2.5.3 Chemical vapour deposition

Different from laser ablation and arc discharge method thermal synthesis method depends on thermal source to produce CNTs by breaking down the carbon source generally with existence of catalysis [70]. High pressure CO synthesis, flame synthesis, chemical vapour deposition (CVD), and plasma enhanced chemical vapourdeposition (PECVD) synthesis are methods using thermal source to produce CNTs. Chemical vapour deposition method is deposition of a hydrocarbon gas as carbon source (i.e. acetylene, methane etc.) on a metal catalyst (Fe, Co, Ni, Pd etc) at temperatures between 500 and 1200 ºC. CVD has been used for production of nanofibers for long time till Yacaman et.al used it for production of CNT. CVD is preferred for CNT syntheses for high purity and large scale production. CVD which was first reported to produce MWCNTs by Endo et al., can synthesise both SWCNTs and MWCNTs. One of the main challenges in CNT production, which is CVD method with existence of catalysts is maintain mass production and low cost. In this respect, the catalytic method is claimed to be best because of lower reaction temperatures and cost [71]. Moreover, the amorphous carbon produced during the thermal decomposition of hydrocarbons can be eliminated by purification.

CNT production by CVD can be either on a fixed bed or fluidized bed reactor. In fixed bed CVD method as shown in Figure 2.6, the furnace placed horizontal to the ground and the quartz tube is placed in it. The substrate material (MgO, alumina, zeolite etc.) coated with a catalyst (Fe, Co, Ni, Ag, Ti, etc.) is placed in the quartz tube and fed by a carbon source (i.e. hydrocarbons). Generally, with existence of an inert gas to maintain continuous gas flow. There are a number of parameters affecting the quality and amount of CNTs synthesis by CVD method.

- Temperature

- Type and amount of the catalyst material

- Type and amount of the substrate material

- Gas flow rate

- Duration of the synthesis

- Diameter of the reactor
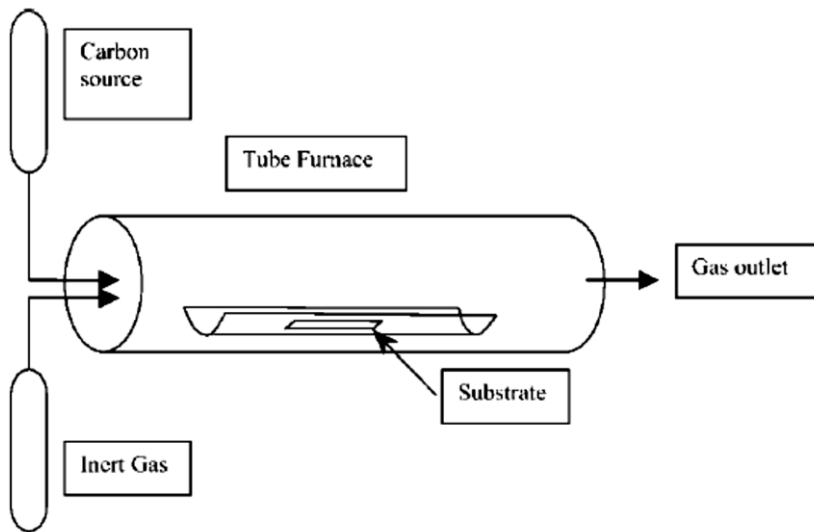
Figure 2.8 : Schematic view of fixed bed CVD reactor.

In fluidised bed CVD method as the interaction area of the carbon source gases and the catalyst increases with fluidisation, large scale production is possible. As shown in Figure 2.7 the furnace is placed vertical to the ground and the quartz reactor is located in it. The substrate & catalyst couple is placed in the hot zone of the furnace, and the gas flow through the reactor is maintained. As the carbon source gas flows through the reactor the catalyst and substrate interacts with the gas and decomposes it for CNT synthesis.
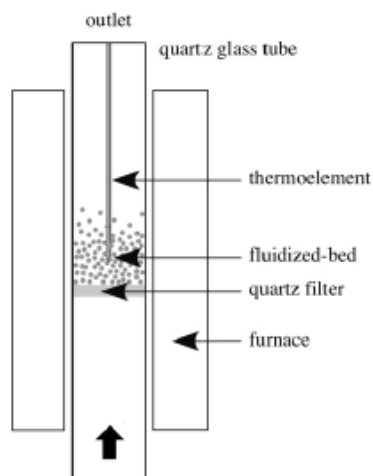
Figure 2.9 : Schematic view of fluidised bed CVD reactor.

3. SEPARATION OF SINGLE WALL CARBON NANOTUBES

3.1 Physical Methods

3.1.1 Ultracentrifugation for SWCNTs separation

Various separation methods have been developed over the last few years to obtain small amounts of SWCNTs with a specific chirality or electronic type. Of all these techniques, the density gradient ultracentrifugation (DGU) method, adapted to SWCNTs by Arnold et al. [72, 73] is considered one of the most promising and effective for achieving good SWCNT selectivity not only by electronic type, but also diameter, and even chirality [73]. Generally speaking, in the DGU method SWCNTs are suspended in water by dispersing with a surfactant, which forms a micelle around the SWCNTs. Different wrapping morphologies form micelles of different sizes and densities, and DGU is used to separate the surfactant-wrapped SWCNTs based on these small density differences. The choices of surfactants and density gradient profile turn out to be very important, with the former playing the most critical role. Additionally, dual-surfactant recipes have been the most effective in isolating SWCNTs [73].

The most commonly used surfactants in DGU are anionic salts such as sodium dodecyl sulfate (SDS) and bile salts such as sodium deoxycholate (DOC) or sodium cholate (SC). These surfactants have different affinities to different SWCNTs because of their specific molecular structures [74].

Density-gradient ultracentrifugation is a method commonly used in biology for separating cellular components with different buoyant densities. The centrifuge tubes containing liquid mixtures are arranged to form a varying density profile before adding sample. Under strong centrifugation, sample components will migrate to different regions that match their individual densities. The separation of SWCNTs by centrifugation is dependent on how surfactant molecules are organized on the surface of the carbon nanotube. DNA, sodium dodecyl sulphate and sodium cholate are common surfactants used in centrifugation separation (Figure 3.1). Hersam and

coworkers demonstrated that by using density-gradient ultracentrifugation, pure semiconducting SWCNTs, such as (6,5) and (7,5), can be separated [75].

Although a few pure SWCNTs have been separated by density-gradient ultracentrifugation, it is difficult to separate nanotube with a similar density. In order to solve this problem, Weisman and coworkers introduced nonlinear density-gradient ultracentrifugation for SWCNT separation [76]. By building a nonlinear density gradient, they successfully separated more than ten different types of pure SWCNTs from raw SWCNT samples which usually only yielded one or two pure SWCNT species.
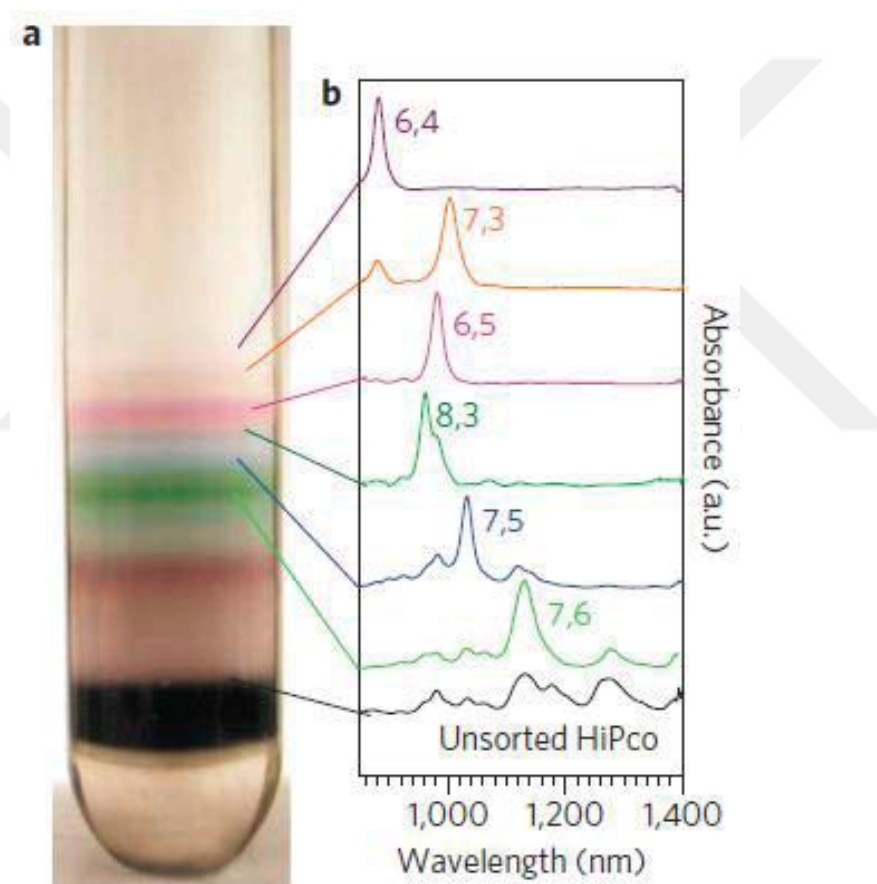
Figure 3.1 : Separation of SWCNT by centrifugation [75].

3.1.2 Gel electrophoresis for SWCNTs separation

Electrophoretic separation is one such class of techniques which have recently been applied for separation of metallic from semiconducting SWCNTs [77,78]. Electrophoretic separation methods apply an electric field to SWCNTs suspended by

a suitable surfactant or dispersant, separating species which carry differential charges by relative motion with respect to each other.

Recently, promising results have been reported using gel electrophoresis for separating the metallic from semiconducting SWCNTs. A study conducted by Tanaka et al [78] showed that metallic and semiconducting SWCNTs may be effectively separated through Agarose gel electrophoresis (AGE) when applied in conjunction with the use of a suitable surfactant. The authors reported that among the various gels and surfactants tested, detectible separation took place only when the combination of sodium dodecyl sulfate (SDS) and Agarose gel was used, demonstrating a gel/surfactant synergy. The reasons for the effectiveness of SDS in Agarose gel electrophoresis of SWCNTs are not clearly understood.
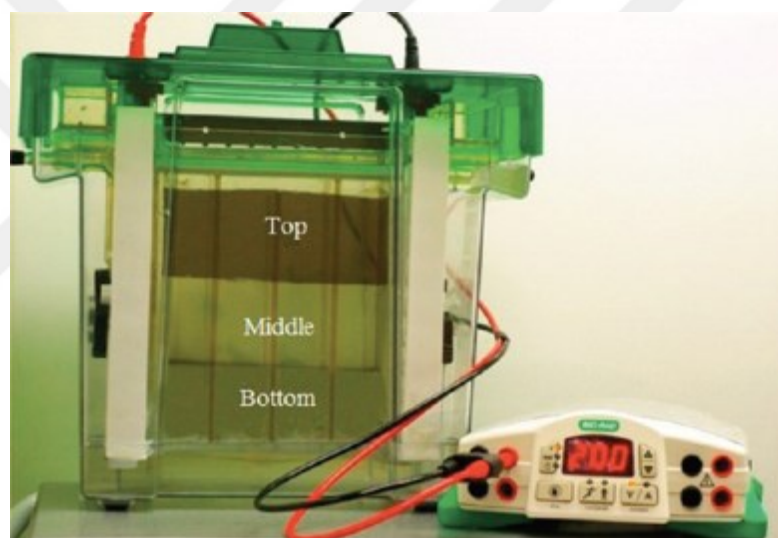
Figure 3.2 : A Agarose gel electrophoresis (AGE) system.

To improve the efficiency of Agarose gel electrophoresis (AGE) in separating nanotubes by metallicity, Sara Mesgari et al. used a chemically preselective dispersant in place of SDS. It has been shown experimentally and theoretically that amine containing compounds preferentially adsorb onto metallic nanotubes [79,80]. They proposed that use of a chemically selective dispersant that preferentially disperses and suspends metallic nanotubes should significantly improve the purity of the separated nanotubes achieved with the inherently high yield AGE process. They found that considerably better separation to obtain 95% semiconducting SWCNTs may be achieved using chondroitin sulfate (CS-A) as the dispersant in AGE, rather than the previously reported SDS. This work extended the use of CS-A to metallicity-

based separation of SWCNTs, specifically using arc discharge SWCNTs. The effectiveness of CS-A for AGE separation to achieve higher separation efficiency than SDS was demonstrated by ultraviolet− visible-near-infrared (UV− vis- NIR) spectroscopy, Raman spectroscopy and field effect transistor results. The separation yield achieved with CS-A assisted AGE was also rather high (25%).

Finally, they reported on the considerably better separation achieved using chondroitin sulfate (CSA) as a dispersant in AGE compared with SDS-assisted AGE. The CS-A assisted AGE technique may be used to produce in a single pass semiconducting SWCNTs with purity of 95%, compared with 85% purity achieved with SDS-assisted AGE for the same arc discharge nanotubes. Further, the yield of CS-A assisted AGE is about 25%, which is in the order of 5 to 10 times the yields of other reported highly selective techniques. Semiconducting SWCNTs produced via CS-A/AGE were used to fabricate field effect transistors (FET) with mobilities of ∼ 2 to 8 cm^2 / (V s) and on/off ratios from 10^2 to 10^5, which are significantly higher than the mobility of 0.7 cm^2 /(V s), and on/off ratio of 10^4 reported for FETs made with semiconducting SWCNTs produced by SDS-assisted AGE. The excellent yield-cum-purity single-pass separation is achievable with this unique chemically selective CS-A dispersant with AGE because of its ability to wrap the nanotubes well, high degree of sulfation making the nanotube/CS-A hybrid highly charged and amine functionality resulting in preselectivity of metallic nanotubes, causing the latter to migrate much more effectively under a uniform electric field.
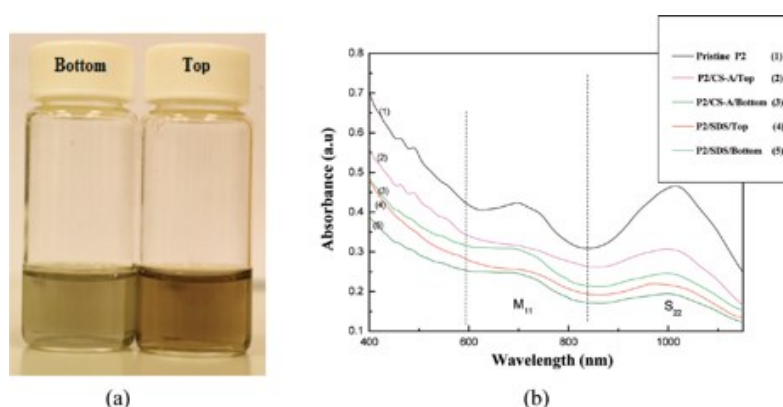
Figure 3.3 : (a) The bottom fraction of the gel (greenish) is enriched in metallic SWCNTs while the top fraction of the gel (pinkish) contains predominantly semiconducting nanotubes. (b) UV−vis-NIR spectra of P2/Pristine, P2/CS-A, and of P2/SDSgel fractions after gel electrophoresis [81].

3.2 Chemical Methods

3.2.1 Gel chromatography for SWCNTs separation

Gel chromatography has been present as an effective method for separation of metallic and semiconducting carbon nanotubes when starting with dispersing in sodium dodecyl sulfate (SDS). The efficacy of the surfactant concentration in this process has been examined for chromatographic separation using a dextran-based gel as the stationary phase. Reducing the concentration of SDS from 4 to 0.5 wt.% caused a slow, increase in the adsorption of semiconducting nanotubes to the gel, with low concentrations of SDS (around 0.5%) found to provide the best semiconductor–metal separation. The concentration of SDS is found to have a critical influence on the metal–semiconductor separation efficacy for chromatography of CNT dispersions in Sephacryl gel. Low concentrations around 0.5% SDS facilitate better metal–semiconductor separation. As the concentration of SDS is increased, the strength of the adsorption interaction between semiconducting species and the gel begins to decrease, with larger diameter species affected first. The elution order for nanotube species was found to correlate weakly with diameter, but strongly with local curvature radius and nanotube family parameters. This suggests a lower density of surfactant coverage on nanotubes with higher bond curvature [82].

However, despite the obvious importance of understanding the underlying mechanism behind such separation, there is still a distinct lack of knowledge in this area that makes their optimization quite difficult. There have been a number of researchers exploring the development of scalable and reproducible SWCNT separation technologies, though chromatography has proven to be one of the more popular techniques. For example, several research groups [83-85] have reported length separation by using the size-exclusion chromatography, whil st Liu et al [86] presented a method for the chirality separation of SWCNTs suspended in sodium dodecyl sulfate (SDS) using multicolumn gel chromatography.

The size-exclusion effect is a simple separation concept that larger molecules are eluted faster than smaller ones. In the case of SWCNTs, longer nanotubes elute faster than shorter tubes due to their larger volume/shape and higher molecular weight. Moshammer e t al. successfully separated M- and S-SWCNTs using an allyl dextran-based size-exclusion gel (Sephacryl S-200, GE Healthcare) [87].

23

Kataura and coworker further optimized this method by attachting different gel column together to achieve large-scale separation88 (Figure 3.4).
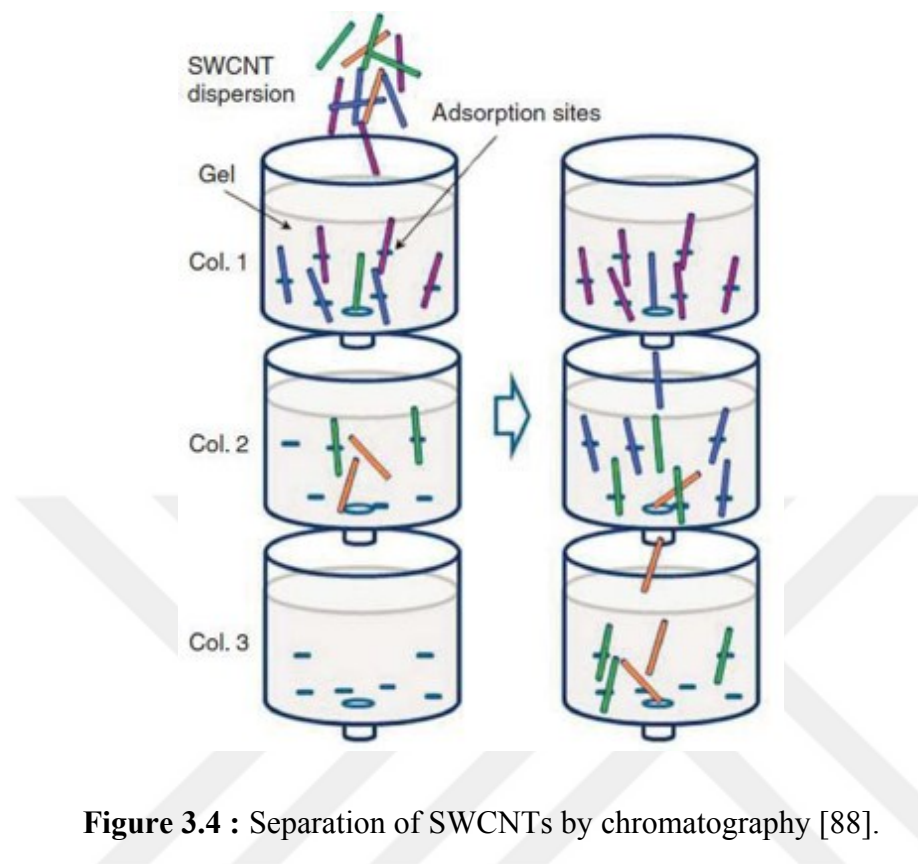
Figure 3.4 : Separation of SWCNTs by chromatography [88].

As recently reported by Hirano et al., in a SDS-stabilized system, s-SWCNTs have higher affinity towards the gel than do m-SWCNTs. Consequently, during the elution, s-SWCNTs adsorb onto the gel to a much greater extent, which results in a longer time to flow through the gel than m-SWCNTs [89].

In a study the research group used surfactant coverage guiding principles to establish methods of using mixed surfactants in the separation of carbon nanotubes via the gel-based method. They first establish the protocol used to enable various mono surfactant separations. Then they study the concentration dependent effect of mixing various bile salt surfactants with SDS. They examined a few commonly used surfactants for these systems, sodium dodecyl sulfate (SDS), sodium cholate (SC), sodium deoxycholate (SDOC), and sodium taurocholate(STC). This study showing that these surfactants is not effective in dispersing nanotubes alone and was determined that SDS is the best for separating SWCNTs. (Figure 3.5)
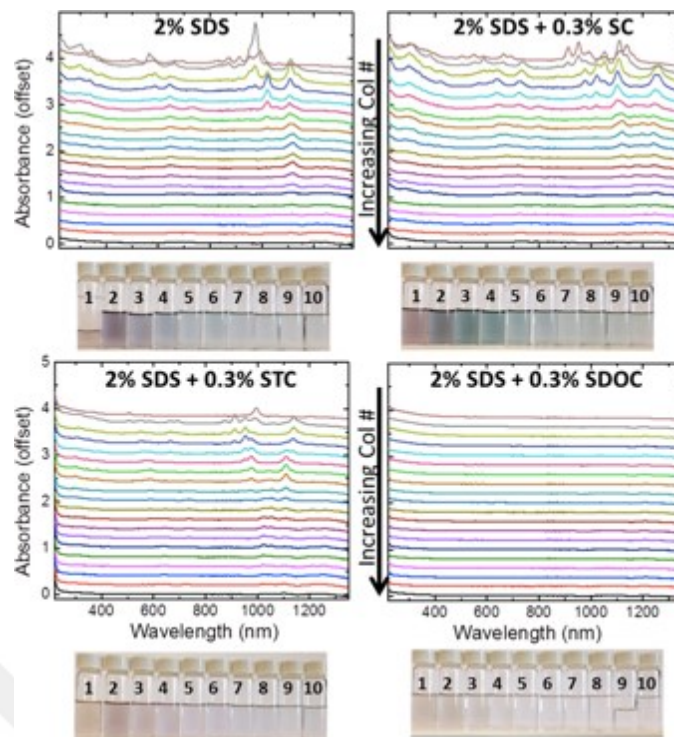
Figure 3.5 : Absorbance result of chromatography with % 2 SDS, % 2 SDS + % 0.3 SC , % 2 SDS + % 0.3 STC, % 2 SDS + % 0.3 SDOC [93].

Several studies from the Kataura, Doorn, and other groups related to altering the SDS phase around the tube have used temperature, [90] and pH, [91,92] to manipulate the SDS phase around the tube, these studies also indicate that the adsorption occurs directly between the SWCNT surface and the Sephacryl, where the surfactant mediates the chiral selectivity but not the binding itself [93].

Benjamin S. Flavel in a study after complete separation of m- from s-SWCNTs, the pH of the 1 wt % SDS eluent solution was reduced from pH 7 to 1 in decrements of 1 pH level. Upon reaching pH 4, the trapped s-SWCNTs can be seen to separate into different colored moving eluent bands. The resolution of these bands was then improved upon further reduction of pH, with yellow, green, blue, and purple bands afforded for pH 4, 3, 2, and 1, respectively [94].

They showed with reduction of pH, the originally strong interaction of s-SWCNT could be reduced and allowed for diameter-dependent fractionation. (Figure 3.6)
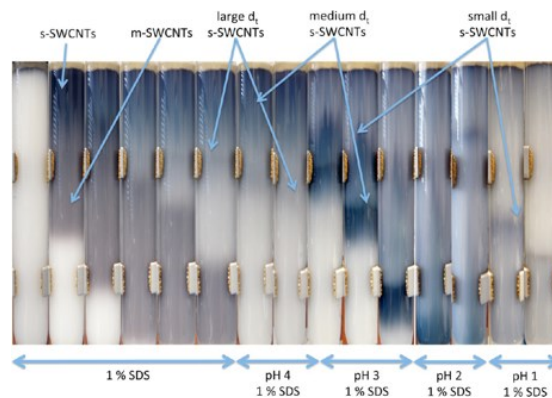
Figure 3.6 : Time lapse photography of HiPCo SWCNTs suspended in 1wt%SDS on a Sephacryl S-200 size-exclusion gel, followed by subsequent reductions of pH [94].

Liu et al. described a method where a larger concentration (5% versus 2%) of SDS elutes the semiconducting SWCNTs and 1% of SDS elutes metallic SWCNTs; but George S. Tulevski et al did it both with 1% of SDS solution, 1% SDS solution (total of ca. 100 mL) is added and is continually added until all of the SWCNTs (now separated) pass through the column. Typical elution times are 30 min for the metallic fraction and 90 min for the semiconducting fraction (Figure 3.7). UV_vis_NIR spectrum of this separation as shown in Figure 3.8. [95].
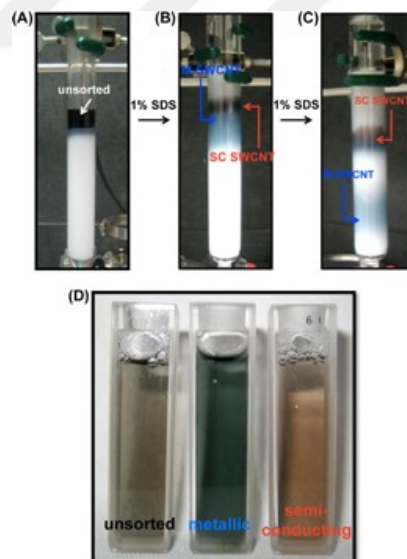
Figure 3.7 : Images of the separation process when the CNT solution is (a) initially loaded (b) beginning to move down the column while forming two distinct bands and (c) near the bottom of the column where a large separation between the bands is observed. The images and labels show how the sc-CNTs move more slowly in the column than the m-CNTs while eluting with the same surfactant mixture. An image of the unsorted, metallic, and semiconducting fractions after separation is shown in panel (d) [95].
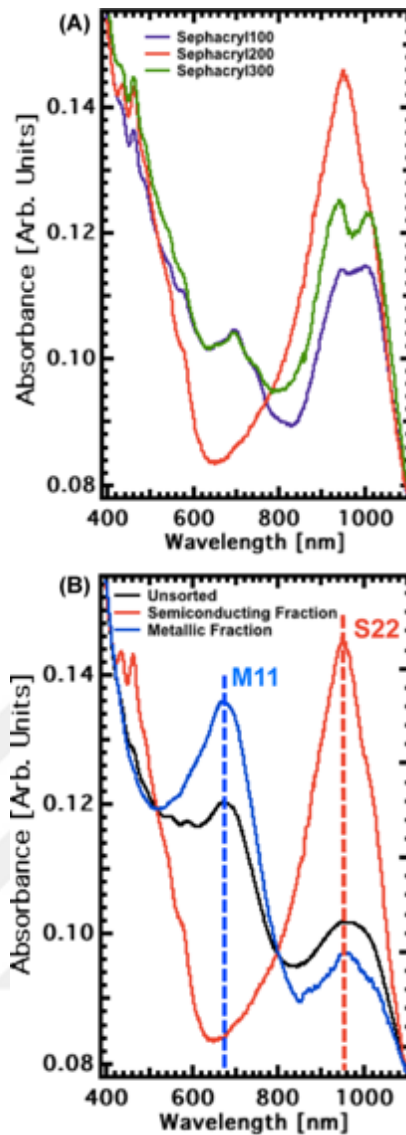
Figure 3.8 : (a) UV_vis_NIR spectrum of the semiconducting fraction after passing the SWCNT solutions through three different column mediums, including Sephacryl-100 (purple), 200 (red), and 300 (green). The pore size of the columns increases with increasing number. The data indicates that Sephacryl 200 yields the highest semiconducting purity. (b) UV_vis_NIR spectrumof theunsorted (black), semiconducting fraction (red), and metallic fraction (blue) after passing [95].

Kataura et. al. reported the chirality and enantiomer separation of metallic SWCNTs using gel chromatography with 0.3-1% of SDS, which has been the last remaining issue in SWCNT separation that has yet to be achieved. The key to the separation is summarized as the following three points: (i) the use of a preseparated metallic SWCNT mixture to eliminate the semiconducting SWCNTs that are more interactive with the gel; (ii) the reduction of the concentration of dispersant to increase the interaction between the metallic SWCNTs and the gel; and (iii) the use of a long

column to increase the number of interaction sites that enhance the slight differences between metallic SWCNT species [96].

3.2.2 Selective adsorption method

3.2.2.1 Using Amines for SWCNTs separation

By taking advantage of amines adsorbing metallic SWCNTs more strongly, Yutaka Maeda and his coworkers have developed a separation method that makes metallic SWCNTs highly enriched. The weakly adsorbed amines are easily removable after separation. This separation method is simple and convenient, suggesting a potential industrial utilization for widespread applications of SWCNTs. They show a separation method involving a dispersion-centrifugation process in a tetrahydrofuran solution of amine- 1M octylamine-, which makes metallic SWCNTs highly concentrated to 87% in a simple way.

In the amine-assisted method, it is important that metallic SWCNTs are more strongly adsorbed by amines than semiconducting SWCNTs and the adsorbed amines are removable after separation [97].

After 5years this group examined this process using various amines in different concentrations. The proportion of m-SWCNTs toward s-SWCNTs increased with an increase of concentration of amines. (Figure 3.9) Also, they found that the separation efficiency of m-SWCNTs depends on amines. (Figure 3.10)
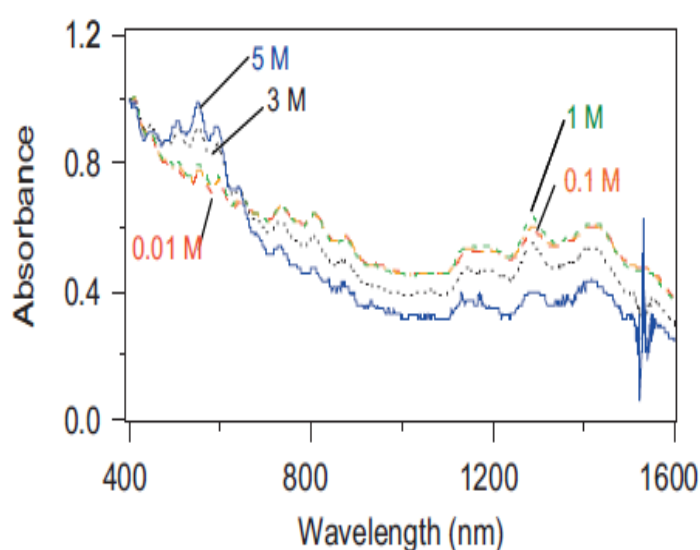
Figure 3.9 : Absorption spectra of supernatant solution of SWCNTs treated in different concentration of octylamine [98].

28

amine	0.01 M	0.1 M	1 M	3 M	5 M
isopropylamine	1.00	1.04	1.05	1.21	1.81
propylamine	1.02	1.04	1.06	1.07	1.13
dipropylamine	1.00	1.01	1.03	1.19	1.33
tripropylamine	1.00	1.00	1.09		
octylamine	1.02	1.02	1.02	1.05	
dioctylamine	1.00	1.00	1.00	1.03	
cyclohexylamine	1.02	1.04	1.04		1.04

Figure 3.10 : Separation efficiency of m-SWCNT in THF solution using various amines in different concentration [98].

SWCNTs thin films were also prepared from the SWCNTs dispersion. The sheet resistance of the SWCNTs films decreased with an increase of proportion of m-SWCNTs. This preparation method for SWCNTs thin films has advantages of control of conductivity by the tuning of proportion of m-SWCNTs. Development of large-scale synthesis methods of SWCNTs and improvement of separation methods of m- and s-SWCNTs opens practical use of SWCNTs.
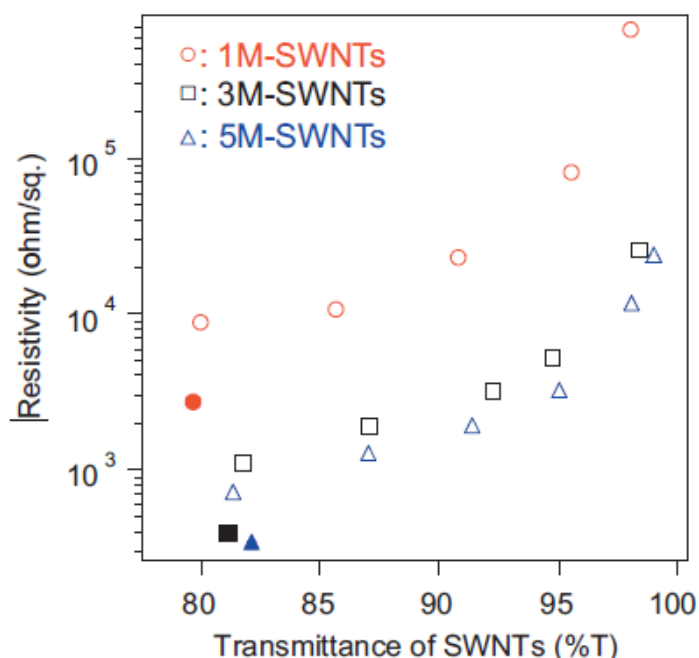
Figure 3.11 : Prepared separated m-SWCNTs thin films resistivity's [98].

The efficiency of separation of metallic SWCNTs was controlled by the amine concentration. With high amine concentration, selective dispersion of metallic SWCNTs was achieved (Fig. 3.12). However, both metallic and semiconducting SWCNTs were dispersed in the supernatant at low amine concentrations. It was proposed that not only the concentration of amines but also the density of amines plays an important role in the selective dispersion of metallic SWCNTs. Microscopic analyses of the supernatant showed that dispersion and centrifugation of SWCNTs in Tetrahydrofuran (THF) containing an amine are effective not only for separation of metallic and semiconducting SWCNTs but also for separation of SWCNTs having different tube lengths [99].
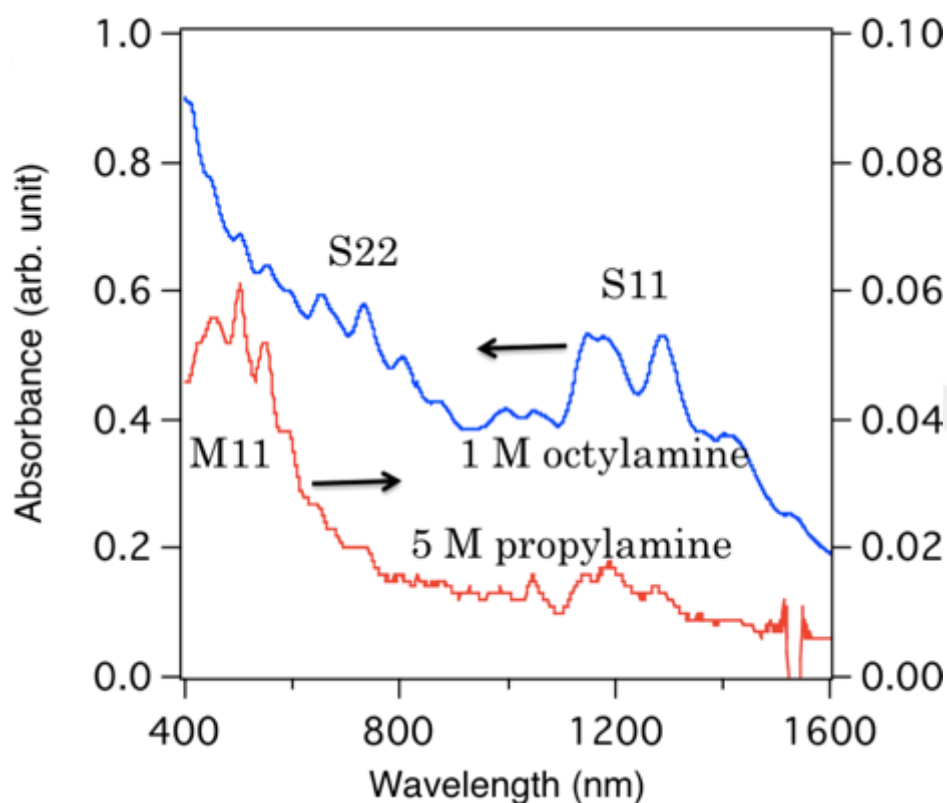
Figure 3.12 : Absorption spectra of supernatant solution of SWCNTs treated in (a) 1M octylamine and (b) 5M propylamine [99].

3.2.2.2 Aqueous two-phase system (ATPS) for SWCNTs separation

Aqueous two-phase system (ATPS) is a very useful technique for proteins purification and recovery [100]. It is a benign and nontoxic separation technique that uses water-soluble, phase separating polymer/polymer or salt/polymer system [101]. One example of a polymer/salt system is polyethylene glycol (PEG)/potassium phosphate, and an example for polymer/polymer system is the PEG/ dextran [102]. ATPS has a few

advantages over other purification methods such as low cost, short processing time and the potential for large scale purification. The factors that influence the outcome of separation includes: type of polymer used; molecular weight (Mw) of the polymer involved; temperature of system; pH of system; and also the addition of salt [103].

To separate SWCNTs using an ATPS, a new ATPS has been developed using PEG, dextran, N-methylpyrrolidone (NMP), cetyltrimethylammonium bromide (CTAB) and water. Dextran has been reported to wrap around SWCNT [104]. PEG is selected for its ability to solubilise in water as well as many types of organic solvents [105]. Organic solvent NMP and cationic surfactant CTAB are known to disperse single-walled carbon nanotubes [106] effectively. The separation of metallic and semiconducting species is due to the attraction between amine and semiconducting species. This affinity is expected to cause the S-SWCNT to move towards amine-rich bottom phase while leaving the metallic species in the amine-poor phase [107].

Malcolm S.Y. Tang et al. separated of m-SWCNT from s-SWCNT by using PEG with different molecular weight i.e. 4000, 6000, 10,000 and 20,000 g/mol. The best separation was achieved using MW of PEG 6000 g/mol at 15% (w/w), coupled with dextran 40,000 g/ mol at concentration 23% (w/w). The highest ratio of M_{11}/S_{22} obtained is 0.2574. They also observed that the difference between yield of metallic and semiconducting species is proportional to the purity of the nanotubes. The results show that molecular weight of PEG and volume ratio could influence the nanotube partitioning. However, partitioning behavior of SWCNT is independent of the changes in volume ratio [108].

3.2.2.3 Using polymer for SWCNTs separation

Organic polymers exhibit their advantages in separating SWCNTs at a lower cost. Most of the polymers used for SWCNT separation are aromatic polymer and its derivatives. The rigid aromatic polymers are found to wrap SWCNT by aligning the aromatic units on the tube surface to maximize the π-π interaction [109]. The aromatic units can be incorporated into the backbone or modified as pendant functional groups. Different kinds of conjugated polymers have been designed and synthesized [110, 111]. There are some examples in Figure 3.13
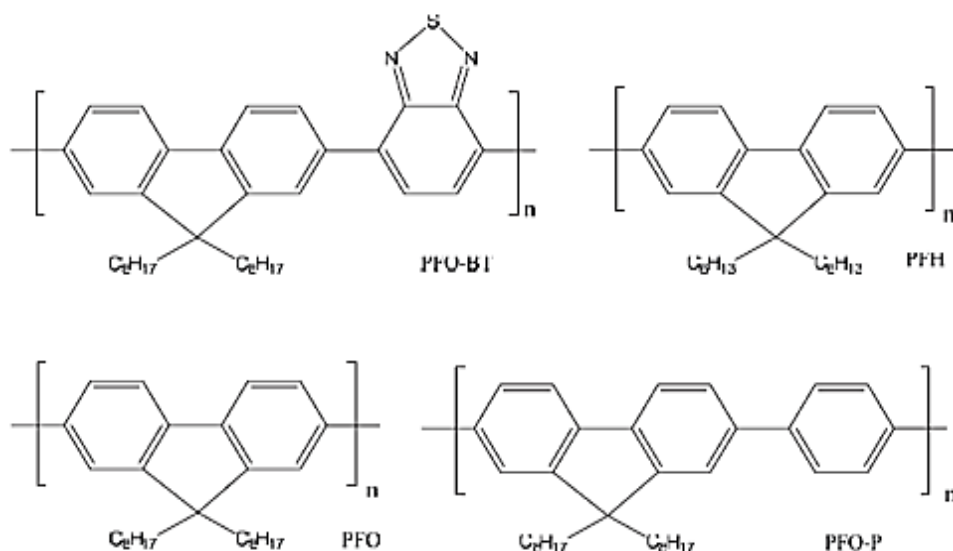
Figure 3.13 : Types of polymer used for SWCNT separation [110].

One example is polymer poly (9,9-dioctylfluorenyl-2,7-diyl) (PFO) which exhibits a particular selectivity of SWCNT (6,5).111 Nicholas and coworkers suggest that the separation selectivity of PFO is related to the chirality angle of SWCNT.111 Interestingly, this selectivity can be changed by introducing heterocyclic unit on the polymer backbone. For example, the polymer PFO-BT exhibits a strong selectivity for nanotubes with diameter around 1.05 nm.

Yusheng Chen et all. Synthesized A water-soluble poly [(m -phenylenevinylene)-alt - (p -phenylenevinylene)] (PmPV 2) which exhibits an unsymmetrical substitution pattern on the para phenylene unit. With one substituent being hydrophilic while the other being hydrophobic, the polymer chain has a higher tendency to fold in aqueous solution, thereby promoting helical conformation. The polymer is found to selectively disperse the single-walled nanotubes (SWCNTs) of small diameters (d =0.75− 0.84 nm), in sharp contrast to PmPV1 with a symmetrical substitution pattern. The intriguing diameter-based selectivity is believed to be associated with the confined helical conformation, which provides a suitable cavity to host the SWCNT of proper sizes. Their study provided a useful demonstration that the polymer conformation can have a profound impact on the SWCNT sorting [112].
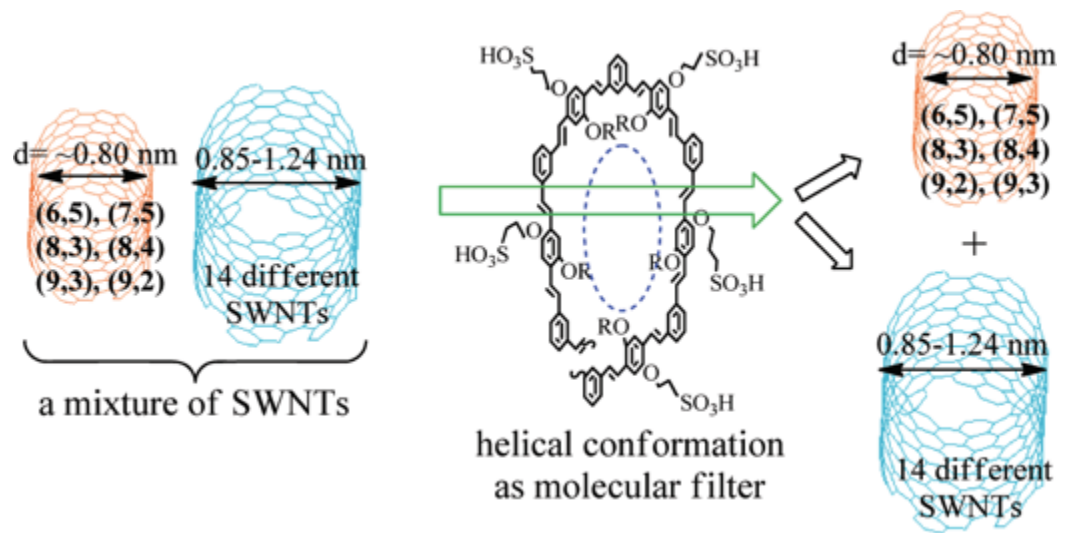
Figure 3.14 : SWCNT size sorting by helical [112].

4. SWCNT CHARACTERIZATION TECHNIQES

To better understand the photophysical properties that are involved in the characterization of SWCNTs it is easiest to think of the simplest model of the density of states. SWCNTs are considered to be m-SWCNTs when an overlapping occurs between the occupied π and unoccupied π^* energy levels allowing electrons to freely move between all the energy levels resulting in conduction [113]. However, in the case of s- SWCNTs, the occupied π and unoccupied π^* orbitals do not overlap resulting in an energy gap. When considering the density of states (DOS) that indicate the number of available electron states at a given energy level, they show regions of extreme density of electrons in very discrete energy levels. These regions are known as van Hove singularities and reflect the 1D nature of SWCNTs [114].

Spectroscopic transitions involve transitions from the valence and conduction band pairs often referred as Ejj. Metallic SWCNTs exhibit a finite amount of electronic states at the Fermi level, while semiconducting SWCNTs result in forbidden regions of electron density between the conduction and valence bands often referred to as bandgaps.

The energy of the bandgap is inversely dependent on the diameter of the SWCNT according to equation 1.4, 1.5, 1.6 [113].

$$E_s{}^{11} = 2aC{-}C\gamma_0/dt \qquad\qquad (4.1)$$

$$E_s{}^{22} = 4aC{-}C\gamma_0/dt \qquad\qquad (4.2)$$

$$E_m{}^{11} = 6aC{-}C\gamma_0/dt \qquad\qquad (4.3)$$

where $aC{-}C$ is the C-C bond length (0.144nm), γ_0 is C-C bond energy (~2.9 eV), and dt is the nanotube diameter. m-SWCNTs generally result in an M_{11} region that lies between ~350 to ~620 nm. s-SWCNTs usually show two main transitions, the S_{11} lying in the region of ~820 – 1700 nm and the S_{22} region lying between ~ 550 – 820 nm (Figure 4.1).
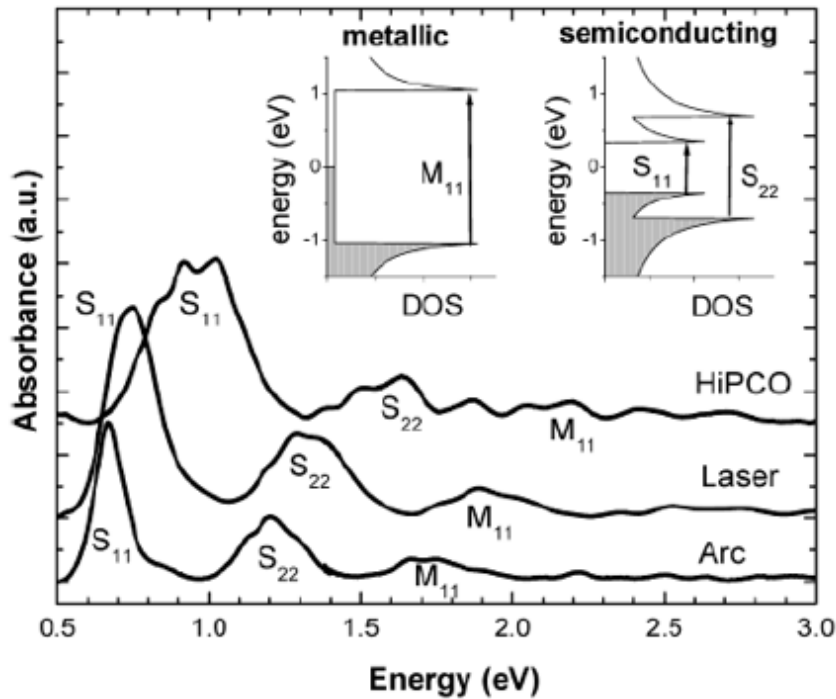
Figure 4.1 : Electronic transitions between the energy bands of SWCNTs with a schematic of the nomenclature designating the interband transitions [115].

After over ten years' development, several analytical techniques have been established to evaluate the purity and chirality of SWCNTs. Those analytical techniques reflect the unique property of different SWCNTs, such as diameter or absorption wavelength. Three common optical measurements will be described below.

4.1 Ultraviolet-Visible-Near Infrared (UV-vis-IR) Absorption Spectroscopy

Absorption spectroscopy of carbon nanotubes is a structure-specific tool widely used for characterization of SWCNT sample composition and purity. Unlike the other ways, absorption spectroscopy has advantage of simultaneous signal detection from all SWCNT species. This is often used to estimate the metallic or semiconducting fraction in SWCNT samples based on the ratio of integrated areas under background-subtracted metallic and semiconducting SWCNT peaks [116]. In addition, absorption backgrounds in SWCNT spectra have been used to evaluate nanotube sample [117]. As a result, absorption spectroscopy provides an efficient approach for chirality and electronic structure-specific assessment of SWCNT samples.

Due to the one dimensional nanostructure, SWCNT has one dimensional electron density of states (DOS) which result in the special optical properties of SWCNT. According to Van Hove singularities, the optical absorption is from electronic

transition from the V_1 to C_1 (first optical transition), or V_2 to C_2 (second optical transition) (Figur 4.2) [118]. One of important optical features of SWCNT is that the absorption is relatively discrete, resulting in different absorptions in UV-vis-NIR range. Thus, it is possible to assign different SWCNTs according to their unique absorption peak.
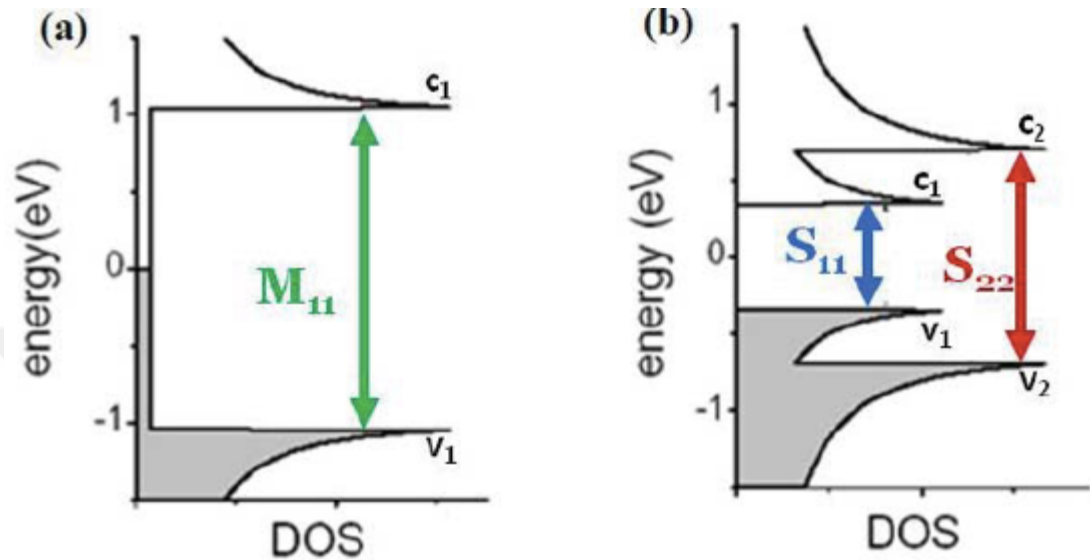
Figure 4.2 : Van Hove singularities of metallic (a) and semiconducting SWCNT (b), where the conduction bands (C_1 and C_2) and valance bands (V_1 and V_2) are indicated along with the density of state (DOS) [118].

Because each SWCNT has a unique interband transition energy, SWCNT can be assigned and classified according to identical absorption peak.118 For example, absorption peak from 900 nm to 1400 nm corresponds to the first optical transition (E^S_{11}) of semiconducting SWCNT; absorption peak from 630 nm to 900 nm corresponds to the second optical transition (E^S_{22}) of semiconducting SWCNT; absorption peaks from 450 nm to 660 nm corresponds to the first optical transition (E^M_{11}) of metallic SWCNT (Figure 4.3). Different interband transition has special energy absorption, which resulting the different absorption intensity even in the same SWCNT sample. For example, in semiconducting SWCNTs, the absorption intensity of E^S_{22} is weaker than that of E^S_{11} [119].
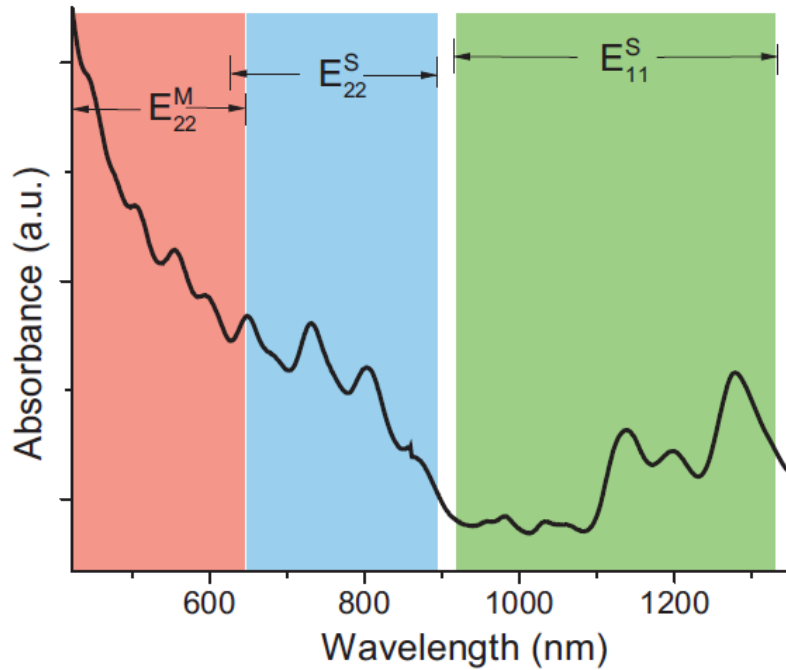
Figure 4.3 : A typical example of UV-vis-NIR absorption spectrum of SWCNTs, which shows absorption peaks of metallic SWCNT (E^M_{11}) and semiconducting SWCNT (E^S_{11}, E^S_{22}) [119].

4.2 Photoluminescence

As mentioned above, SWCNT has interband transitions between its Van Hove singularities. After absorbing energy through the second interband transition, electrons will be excited from the valence band V_2 to the conduction band C_2. During this process, an electron-hole pair (exciton) will be created. The electron and hole will relax from C_2 to C_1 and V_2 to V_1, respectively, followed by recombination through the first transition energy S_{11} (C_1-V_1) which leads to a photoluminescence emission (Figure 4.4). However, this photoluminescence only takes place when the tube is a semiconducting SWCNT. For a metallic SWCNT, although electrons can also be excited to the conduction band by absorbing energy and form electron-hole pair, the hole will not survive for interband relaxing. The electrons in metallic SWCNT will immediately combine with the hole and quench the photoluminescence.

38
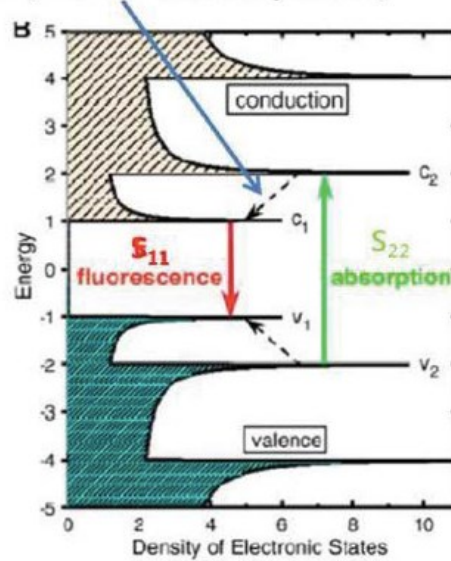
Figure 4.4 : Photoluminescence mechanism of SWCNT [120].

Due to the unique interband energy of semiconducting SWCNT with different chirality, the special excitation and emission wavelength can be used to identify SWCNT. As-prepared raw SWCNTs are a mixture of different kinds of tubes. When the excitation wavelength is scanned in a certain range, the emission intensity can be plotted into a 2D photoluminescence map as a function of excitation and emission wavelengths (Figure 4.5). Each peak on the 2D photoluminescence represents one type of semiconducting SWCNT. By using this method, one can indentify various SWCNTs and detect the intensity distribution of SWCNTs.
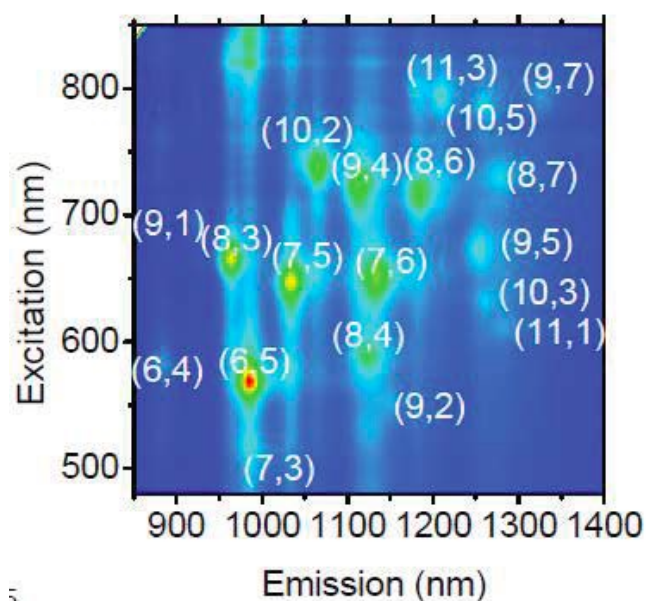
Figure 4.5 : 2D photoluminescence map of SWCNT [121]

39

4.3 Raman Spectroscopy

Besides UV-vis-NIR and 2D photoluminescence, Raman scattering spectroscopy is another useful tool in carbon nanotube's research. Rao and coworker did some pioneering works to prove the Raman scattering phenomenon in SWCNTs [122]. They found SWCNTs with special diameter can be detected in Raman spectroscopy by using a laser with certain wavelengths as an excitation source. This detection depends on both excitation wavelength and diameter of SWCNT. In other words, SWCNTs with a particular diameter can only be excited by a laser with an energy matching its inter band transition. The displacement of a carbon atom on the carbon nanotube is Raman active, which can be detected by different modes of Raman spectroscopy. Three important modes are commonly used in nanotube study: Radial Breathing Mode (RBM), G band Mode and D-band Mode (Figure 4.6)

Raman spectroscopy offers a different way of characterization: carbon nanotubes were found to have diameter-specific radial breathing mode vibrations that are active and may be resonance-enhanced in Raman. Therefore, knowing the frequencies of the breathing mode Raman peaks, one can determine the diameters of carbon nanotubes that are present in the sample and have electronic resonances near the Raman laser wavelength.
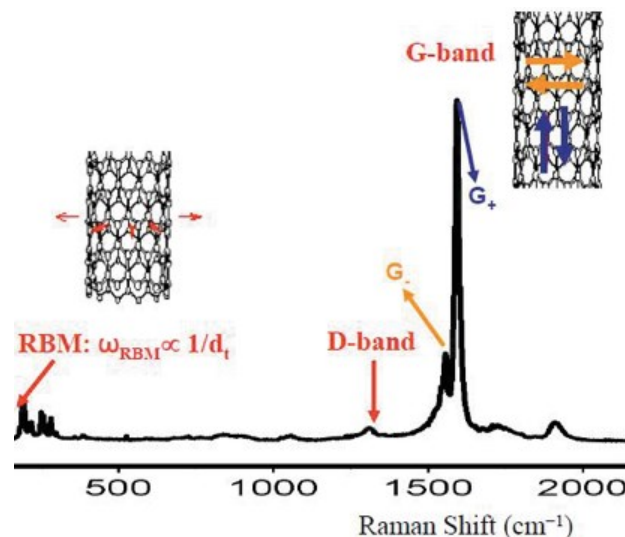
Figure 4.6 : Raman spectroscopy of SWCNT [123].

4.3.1 RBM mode

In RBM mode, carbon atoms vibrate in the radial direction of tube axis, as if the nanotube was breathing, therefore it is called Radial Breathing Mode (RBM). The RBM Raman shift is from 100 to 350 cm^{-1}, which is anti-proportional to the diameter of the detected SWCNT. This relationship is described as: $\omega(RBM) = 219.3/d + 14.7$, where $\omega(RBM)$ is the RBM Raman shift and d is the diameter of carbon nanotube. Because SWCNT with special diameter can only be excited by a laser with matched wavelength, the assignment of SWCNTs can be plotted into a map with functions of excitation energy of laser and tube diameter, which is known as Kataura plot (Figure 4.7).
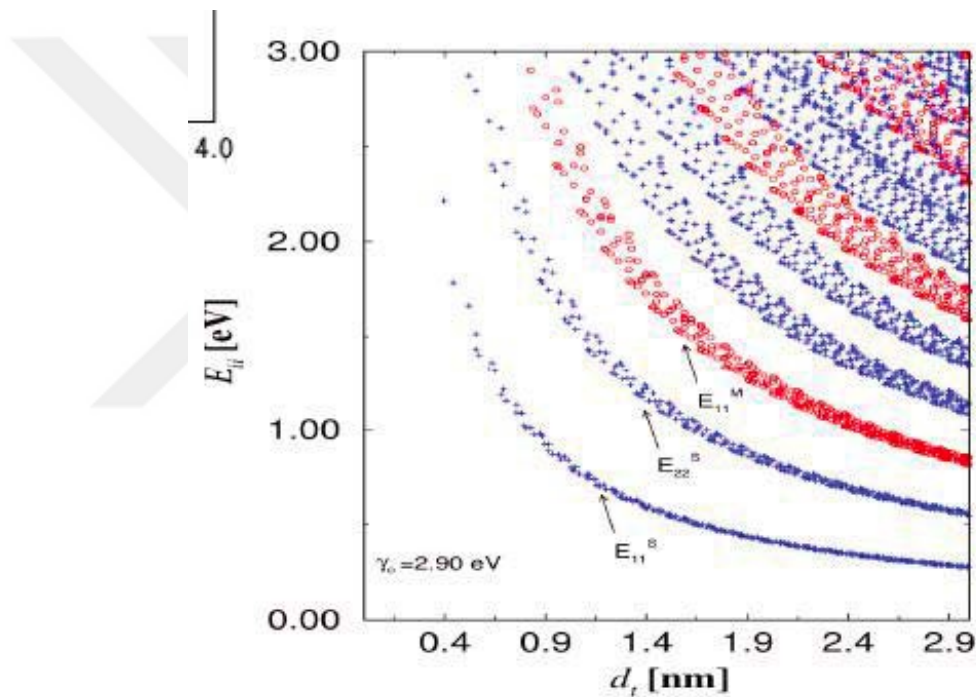
Figure 4.7 : Kataura plot of SWCNTs [123].

4.3.2 G band

G band mode consists of a couple of peaks from 1560 to 1600 cm^{-1}. Those peaks are dependent on several factors: the confinement of phonon wave vector and asymmetry effects according to SWCNT curvature. Two peaks around 1570 cm^{-1} and 1590 cm^{-1} are identification of semiconducting and metallic SWCNT, which are called G$^-\Box$ and G$^+$ respectively. G$^-$ band is related to the vibration of carbon atom along the circumferential direction of tube, whereas G$^+$ band describes the vibration of carbon

atom along the nanotube axis. Generally speaking, a broad and high G$^-$ band is a sign of enrichment of metallic SWCNT.

4.3.3 D band

D band appears around 1350 cm^{-1}, which originates from the defect on the SWCNT structure. The defect usually results from the damage of sp^2 structure in SWCNT. The intensity ratio between D band and G band is a good indicator for the purity of SWCNT. If the surface of SWCNT is modified with some functional groups, corresponding D band is expected to be increased, because the modification disturbed the sp^2 hybridization or damaged the integrity of the tube.

5. EXPERIMENTAL STUDIES

5.1 SWCNTs Preparation

SWCNTs used in this study were synthesized by high-pressure catalytic carbon monoxide (CO) (HiPco) decomposition (HiPco, 1.0 ± 0.2 nm) that were purchased from NanoIntegris Inc. HiPco processes generally require high temperature (900 ^{0}C to 1100 ^{0}C) and high pressure (30 to 50 atmospheres) conditions in a customized vessel. A carbon source CO of flows past catalytic clusters of iron and iron pentacarbonyl ($Fe(CO)_5$) as the catalyst and the mixture is injected into the reactor through an insulated, air- or water-cooled stainless-steel injector tipped with a copper nozzle. The $CO/Fe(CO)_5$ mixture rapidly heats and mixes with the shower of carbon monoxide. The clusters formed in situ decompose upon heating. The iron atoms condense into clusters and serve as catalysts, upon which the SWCNTs nucleate and grow. The SWCNTs and iron particles are carried out of the reactor by the hot, dense gas flow into the product collection apparatus. The CO is then recirculated back through the gas flow system and reactor via a compressor, which creates a continuous process. The product contains iron (Fe) nanoparticles and other by-products.

5.2 Separation of SWCNTs by Gel Chromatography

The intrinsic properties of single wall carbon nanotubes (SWCNTs) promote the use of these nanostructures in a wide variety of applications, although their implementation has been limited thus far by the heterogeneous nature of as-produced CNT material. Consequently, the demand for uniformity in nanotube distributions has lead to post-synthesis sorting of SWCNTs being approached in a variety of different ways, with varied levels of success. The high aspect ratio and strong van der Waals cohesive forces of SWCNTs, however, cause detrimental entanglement and bundling. This is a major drawback, as many applications require well-dispersed tubes in order to make full use of their remarkable properties. While each of separation techniques are capable of achieving the m- and s-SWCNTs, selective adsorption on dextran gel or Agarose gel is currently one of the most promising methods for large-scale, high-throughput

43

separations. Nevertheless, novelty of this research relies on using both of Agarose and Sephacryl gels for increasing the efficiency of the separation.

5.2.1 Dispersion

Dispersion of SWCNTs is quite important step for achievement of effective separation. Three main approaches can be pursued to disperse CNTs: (i) use of organic solvents; (ii) covalent attachment of hydrophilic groups to the nanotube surface; and (iii) physical adsorption of amphiphilic molecules (surfactants or polymers). SDS is the surfactant that usually is used for dispersion CNTs. The common factor of SDS for most reported separations suggests this surfactant is highly influential. The mechanism behind the separation is believed to be related to conformational differences between SDS adsorbed on metallic and semiconducting species.

5.2.1.1 Ultrasonication

The first step toward the separation is to disperse SWCNT bundles. Dispersion procedure is as follows: 15 mg of SWCNTs (HiPco, NanoIntegris) was added to 15 ml of deionized water (DI water) with 1 wt % SDS of then sonicated using an ultrasonic homogenizer (BandelinSonopuls ultrasonic homogenizer) equipped with a 0.5-inch. Flat tip for 2 h at a power density of 20 W cm^{-2}, to prevent heating during sonication, the bottle containing the sample solution was immersed in a bath of cold water (5-10°C).

5.2.1.2 Ultracentrifugation

To remove the residue of catalytic metal particles, nanotube bundles and impurities, the dispersed sample solution was centrifuged at 50.000 *rpm* for 2h in a swinging-bucket rotor (Beckman Coulter's Optima™ MAX, Optima MAX-E). The upper 80 % of the supernatant was collected and used for gel chromatography. The resulting supernatant solution and deposit of SWCNTs is designated.
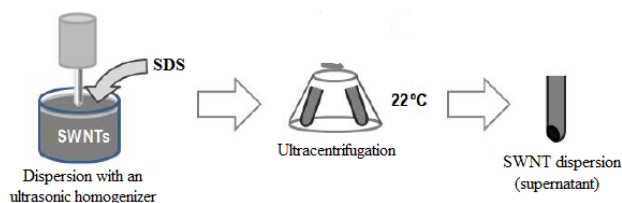
Figure 5.1 : Schematic diagram of the SWCNT/1 wt% SDS dispersion solution at 22 °C.

5.2.2 Gel chromatography

In gel chromatography method, dispersions of nanotubes in the surfactant sodium dodecyl sulfate (SDS) are passed through a gel matrix which is usually composed of Agarose or cross linked allyl dextran gel beads(Sephacryl). For achieving high yiled separation, we used both of these gels consequently.

5.2.2.1 Gel chromatography by using Sephacryl gel

Glass column (20 cm in length and 1.5 cm in inner diameter) were used for the chromatography. Allyl dextran-based size-exclusion gel (Sephacryl gel, S-200 (5-250 kDa) SigmaAldrich) was utilized as the gel media. Gel columns were prepared by filling the same amount of allyl dextran-based size-exclusion gel (1.4 ml of gel beads) into column. The Sephacryl was then washed thoroughly with water to remove excess ethanol and other impurities before being suspended in deionized water (DI water). Then, a 1.4 mL stationary bed of 1 % wt SDS equilibrated Sephacryl S200 gel and 5 ml aliquots of the SWCNT dispersion were applied to column. Next, 1 % wt aqueous SDS solution was used to elute the metallic and unbound nanotubes until no nanotubes were detected in the eluent. To obtain metallic SWCNT, 1 % wt SDS (10ml) was used until no nanotubes were detected in the eluent. The s-SWCNTs adsorbed on the column were desorbed and collected by injection with a 5 % wt SDS (10ml) until no absorbance was detected, Then 1% wt SC (10ml) was used to elute the s-SWCNTs adsorbed onto the gel at 5% wt SDS(10ml).

5.2.2.2 Gel chromatoghraphy by using Agarose gel

The s-SWCNTs adsorbed on the column were desorbed and collected by injection with 5% SDS(10ml) and 1% SC (10ml) until no absorbance was detected (two runs), then all this processes are applied with Agarose gel. According to optical absorbance spectra of separated s-SWCNT, only small s-SWCNTs are adsorbed to dextran gel beads and large s-SWCNTs are adsorbed to Agarose gel beads. Considering these properties, our group have developed a novel mixed method for separation of m-SWCNTs and s-SWCNTs by using dextran and Agarose gels respectively.
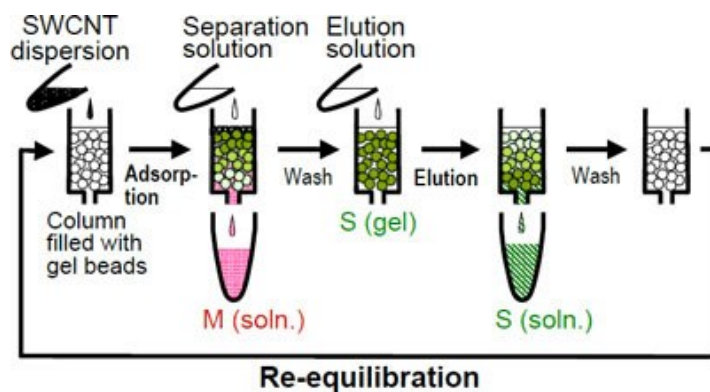
Figure 5.2 : Schematic view of chromatography processes.

The selective adsorption of m/s-SWCNTs in a gel column occurs that related to the gel matrix and surfactant concentration, SWCNTs interact with gel in different ways. By applying SWCNTs/SDS dispersion to a column containing dextran based gel, small s-SWCNTs observed to be adsorbed to the gel and collected by changing the eluent. This process was repeated for obtained unbundle solution until there was no any absorption to the gel. Subsequently, the operation continues with Agarose gel beads for absorbing the large s-SWCNTs repeatedly until the end of adsorption process (two times).

Consequently, we are separated nearly all of the small and large s-SWCNTs and m-SWCNTs that passed through the final column as unbundle solution.

5.2.2.3 Enrichment m-SWCNTs

In chromatography process, after complete separation of m-SWCNTs with applied 1 wt % SDS were not observed pure m-SWCNT, it is why that we applied this solution to second column for removing resedual s-SWCNTs and reached pure m-SWCNTs. For this purpose, after applying m-SWCNs to Sephacryl gel column, 1 % wt SDS solution was used to elute the metallic and unbound nanotubes until no nanotubes were detected in the eluent. The s-SWCNTs adsorbed on the column were desorbed and collected by injection with a 5 % wt SDS (10ml) until no absorbance was detected.

5.3 Characterization of Separated SWCNTs

Metallic and semiconducting SWCNTs characterization was measured by UV-vis NIR, Raman spectrophotometer.

5.3.1 Optical absorption measurement (UV-vis-NIR)

Optical absorption data were recorded from 200 to 1,350 nm with an UV − vis − NIR spectrophotometer (SHIMADZU UV-3150) using a quartz cell with a path length of 5 mm. Pristine HiPco SWCNTs and sorted samples were dispersed in 1 wt % aqueous SDS solution. For the HiPco SWCNTs, the absorption peaks at 850 − 1,350, 500 − 850, 330 − 450 and 300 − 400 nm were derived from the first (S_{11}), second (S_{22}), third (S_{33}) and fourth (S_{44}) optical transitions of the semiconducting SWCNTs. The absorbance peak at 400 − 650 nm represented the first optical transition of metallic m-SWCNTs (M_{11}). The absorption peaks observed in the shorter wavelength region (200 − 300 nm) indicate the UV optical absorption characteristic of the nanotubes.

Figure 5.3 : UV − vis − NIR spectrophotometer (SHIMADZU UV-3150).

5.3.2 Raman spectra measurements

Raman spectra were measured in aqueous SDS solution at a concentration of 1 wt % using a triple monochromator (Bunkou-Keiki, M331-TP) equipped with a charge-coupled device detector. The samples were excited at excitation wavelengths of 514 nm using a power of 10 mW.

Figure 5.4 : Raman spectrophotometer.

6. RESULTS AND DISCUSSIONS

6.1 Characterization of SWCNTs synthesis by Hipco method

HiPco SWCNTs were characterized using transmission electron microscopy (TEM), Raman spectroscopy and thermogravimetric analysis.

TEM enables the analysis of a material in a range of 0.01 μm to 10 μm, retaining the necessary resolution to distinguish surface properties. Accordingly, individual SWCNT mean diameter is approximately 1.0 nm arranged in crystalline bundles which is measured by Unidym from TEM micrographs (Fig. 6.1).
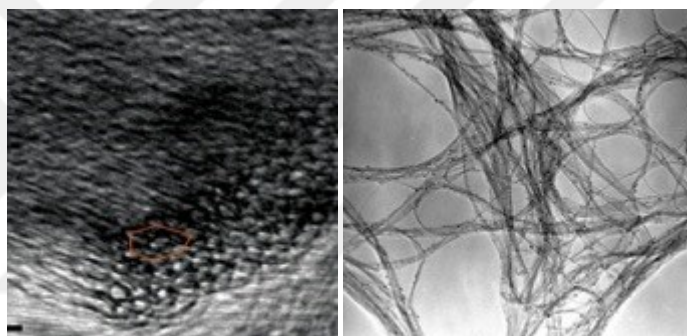
Figure 6.1 : TEM images of Hipco SWCNTs.

Raman spectroscopy is a powerful technique for the characterization of the structure of carbon nanotubes. Figure 6.2 shows Raman spectrum for carbon deposits excited by 633 nm laser. The Raman spectrum of the HiPco SWCNTs contains peak which is special to single wall in radial breathing mode (RBM). The Raman spectrum also shows the characteristic peaks at 1200-1400 cm^{-1} (D band) and 1580-1600 cm^{-1} (G band) for SWCNTs grown on the catalyst. The G and D bands related to the degree of graphitization and the defects in SWCNT structure, respectively. The lower the ratio (I_D/I_G) in the spectrum refers to the lower content of amorphous carbon and defect formation in the structure. Considering this ratio is quite low in our SWCNT sample, amount of amorphous carbon and defect formation is very low.
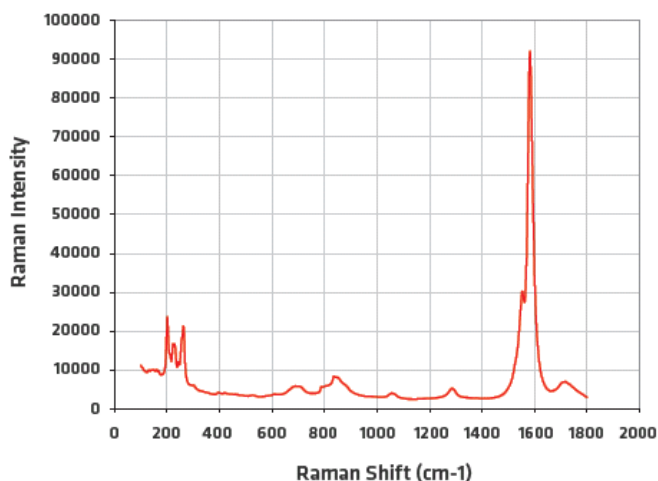
Figure 6.2 : Raman spectroscopy of Hipco SWCNTs.

Thermogravimetric analysis (TGA) is an analytical technique to determine a materials thermal stability by monitoring the change in mass as the specimen is heated. The measurement is carried out in air or inert atmosphere (i.e. Ar, He). The mass of a sample is recorded as a function of time or temperature when the sample is heated/cooled with constantly increasing/decreasing temperature. In the case of CNTs the mass change in a result of oxidation of carbon in the air into carbondioxide and mass gain due to oxidation of the metal catalyst into solid oxides analysis of synthesized SWCNTs was conducted in air atmosphere with 800 °C (Fig. 6.3). The reported figures assume that the residue is present in the product as elemental Fe, and that it is fully converted to Fe_2O_3 during the TGA analysis. Hence, the TGA residual as measured is less than 15 wt %.
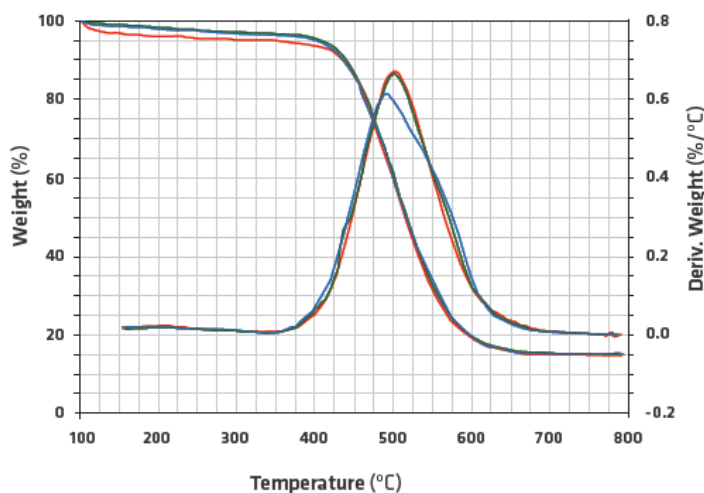
Figure 6.3 : TGA Profile of Hipco SWCNTs.

6.2 Theory Behind Separation and result

For this study, Hipco SWCNTs were selected because of the ability of Hipco process to produce a sample with a small diameter range SWCNTs (1.0 ± 0.2 nm) Sodium dodecyl sulfate (SDS) is responsible for the creation of micelles around individual SWCNTs during sonication, an effort that interferes with the attractive forces in between SWCNTs originally produced in bundles. The hydrophobic tail of the surfactant is what interacts with the SWCNT. This is due to the fact that the SWCNT is a carbonaceous material and is hydrophobic in nature. Larger diameter SWCNTs have more SDS on the surface of the tube than smaller diameter tubes. The correlation between the amount of SDS on the surface of the nanotube and the diameter of the nanotube results in a change in affinity of the semiconducting SWCNTs to the Sephacryl and Agarose gels.

By increasing the concentration of SDS in the mobile phase, the adsorbed SWCNTs are released from the gel by increasing the amount of repulsion the surfactant applies between the SWCNT and the Sephacryl and Agarose gels.

6.2.1 Adsorbing small diameter semiconducting SWCNTs to Sephacryl gel

Figure 6.4 shows Sephacryl gel chromatography processes. Gel column was prepared by filling of 1.4 ml of Sephacryl (allyl dextran-based size-exclusion) gel. 1% wt aqueous SDS solution was used to elute the metallic and unbound nanotubes until no nanotubes were detected in the eluent. To obtain metallic SWCNT, 1% wt SDS (10ml) was used until no nanotubes were detected in the eluent. The s-SWCNTs adsorbed on the column were desorbed and collected by injection with a 5% wt SDS (10ml) until no absorbance was detected, Then 1% wt SC (10ml) was used to elute the s-SWCNTs adsorbed onto the gel at 5% wt SDS (10ml). Smaller diameter SWCNTs with higher affinity will adsorb more strongly to the column while large diameter SWCNTs will adsorb weakly to the column, thus creating a gradient in the column from smaller diameter SWCNT to larger diameter SWCNTs. SDS was able to elute the metallic SWCNTs with 1% wt SDS while leaving the majority of the semiconducting SWCNTs bound to the column. The small s-SWCNTs were eluted with 5% wt SDS and 1% wt SC. Figure 6.5 indicates that separated m- and s-SWCNT with Sephacryl gel that blue one is small semiconducting and green-brown one is metallic.
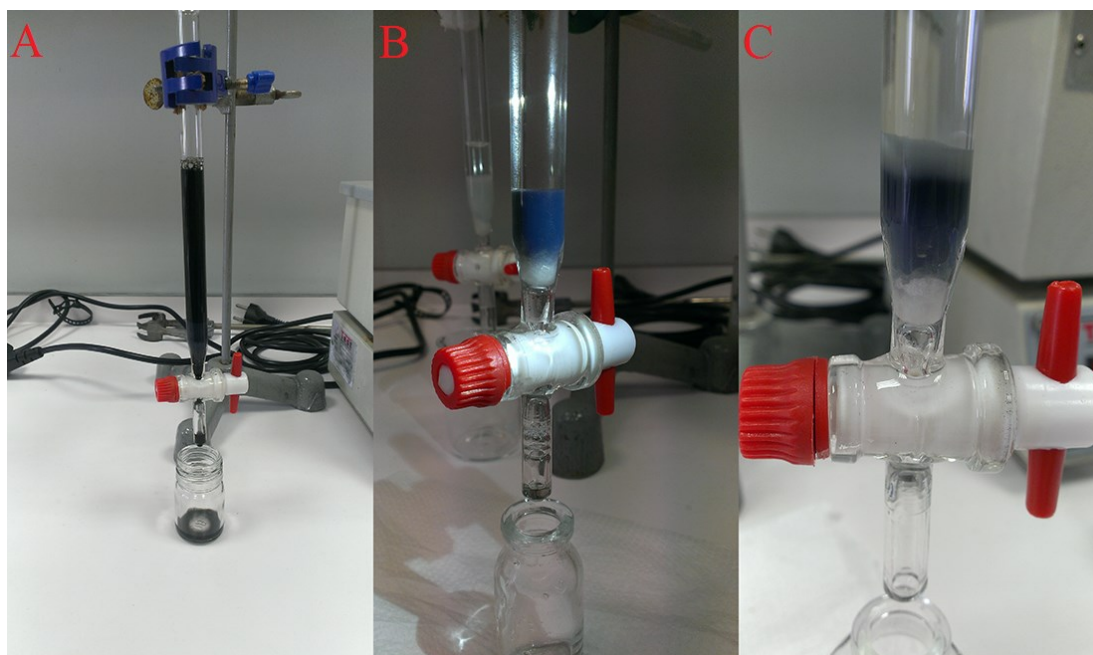
Figure 6.4 : Chromatography processes a) applying sample, b) after applying 1% wt SDS, c) after applying 5% wt SDS.

Figure 6.5 : Separated m- and s-SWCNT with Sephacryl gel (green-brown one is metallic and blue one is small semiconducting).

To determine the compositions of the nanotubes adsorbed, we measured the optical absorption spectra using an ultraviolet-visible-near- infrared spectrophotometer. The optical absorption spectra confirm that the nanotubes adsorbed in each column were enriched with m-SWCNTs and s-SWCNTs. For s-SWCNTs exist different diameter distributions. Overall, small diameter s-SWCNTs piks is around 950-1,150 nm and large diameter s-SWCNTs piks is around 1,150-1,350 nm, when applying a gradient of the eluting surfactant to a Sephacryl gel column with semiconducting SWCNTs adsorbed to the gel. It was observed that the large diameter tubes elute from the column whereas small diameter s-SWCNTs adsorbed to the gel. It is obvious from absorption

52

spectra that Sephacryl gel is usefull for separating small s-SWCNTs whereas Agarose gel is functional for separating large diameter s-SWCNTs.

Figure 6.6 indicates the existence of both semiconducting and metallic characteristics in the pristine HiPco SWCNTs after dispersion and centrifuge. For the HiPco SWCNTs, the absorption peaks at 850−1,350, 500−850, 330 were derived from the first (S_{11}), second (S_{22}), third (S_{33}) optical transitions of the semiconducting SWCNTs, the absorbance peak at 400−650 nm represented the first optical transition of metallic m- SWCNTs.
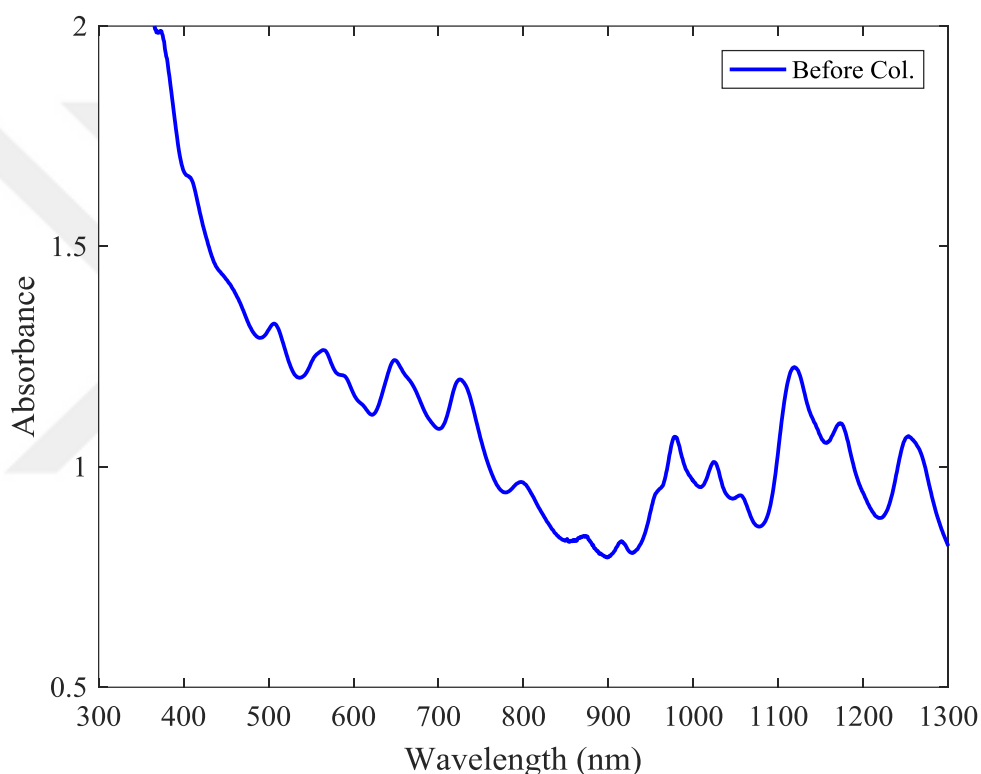
Figure 6.6 : Absorption spectrum of raw Hipco SWCNTs before applying column.

Figure 6.7 shows the absorption spectrum of the sample after 1% wt SDS where a metallic characteristic was mostly expected to be observed but, as can be seen, the s-SWCNTs also exist. Therefore, in order to enrich the metallic part, we repeated the process again for a second column. Section 6.2.3 presents more detail about the method. By this method we obtained purer m-SWCNTs.
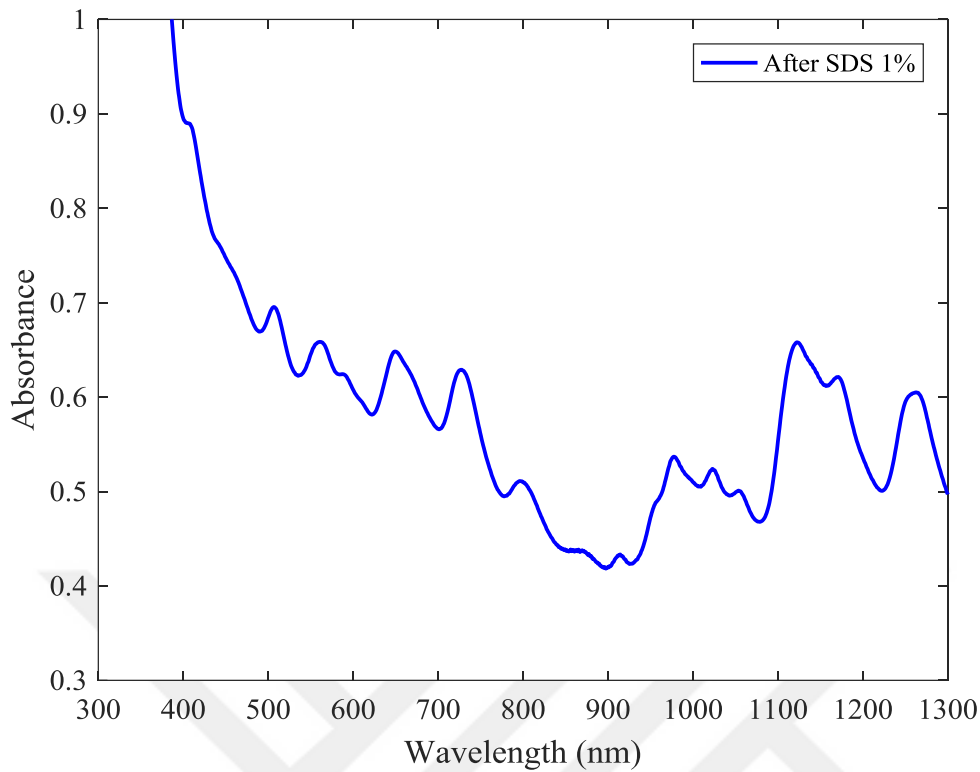
Figure 6.7 : Absorption spectrum after applying SDS 1% in Sephacryl gel.
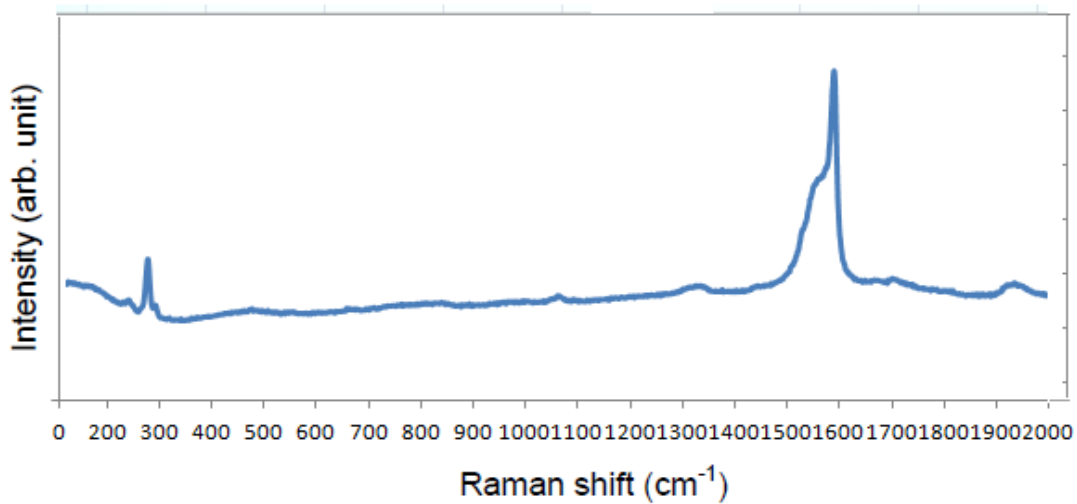
Figure 6.8 : Raman spectrum of solution of after applying 1% wt SDS in Sephacryl gel.

Figure 6.9 shows the absorption spectra of the sample after 5% wt SDS for two consequtive column of Sephacryl gel. Accroding to literature studies (Figures 6.10 and 6.11) [26, 124] it can be inferred that few chiralities of small s-SWCNs which were adsorbed by the gel, were finally eluted by 5% wt SDS; hence the separation is now

completed. It should also be mentioned that the gel chromatography process was repeated for increasing the efficiency by further adsorbing of small s-SWCNTs to the gel inside the column.
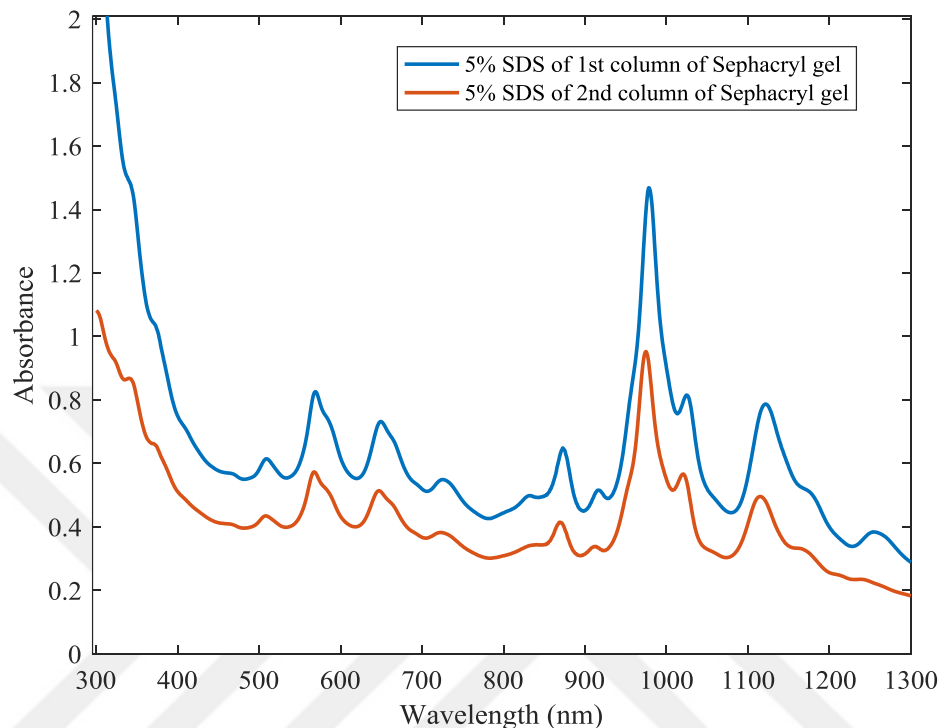
Figure 6.9 : Separated small diameter s-SWCNTs that applied 5% wt SDS in Sephacryl gel for two times.

Figure 6.10 shows the optical absorption spectra of the nanotubes collected from the various columns and that of the unbound metallic nanotubes, with the spectrum of pristine HiPco SWCNTs provided as a reference. These absorption spectra confirm that the nanotubes bound in each gel column were highly enriched with semiconductor nanotubes, whereas the unbound nanotubes were highly enriched with metallic nanotubes. Moreover, for the S-SWCNT fractions from the first to the last column, the E_{11} optical absorbance peaks in the range of 850 − 1,350 nm shift towards longer wavelengths, indicating that the nanotubes with smaller diameters interacted more strongly with the gel and were initially adsorbed on the gel column; this effect resulted in the separation of S-SWCNTs based on their diameter and bandgap. Also, the various S-SWCNT fractions exhibited significant differences in their diameter and chirality distributions. Figure 6.10 shows chirality of small diameters (d = 0.75−0.84 nm) and large diameter (d = 0.85−1.24 nm) single-walled nanotubes (SWCNTs).
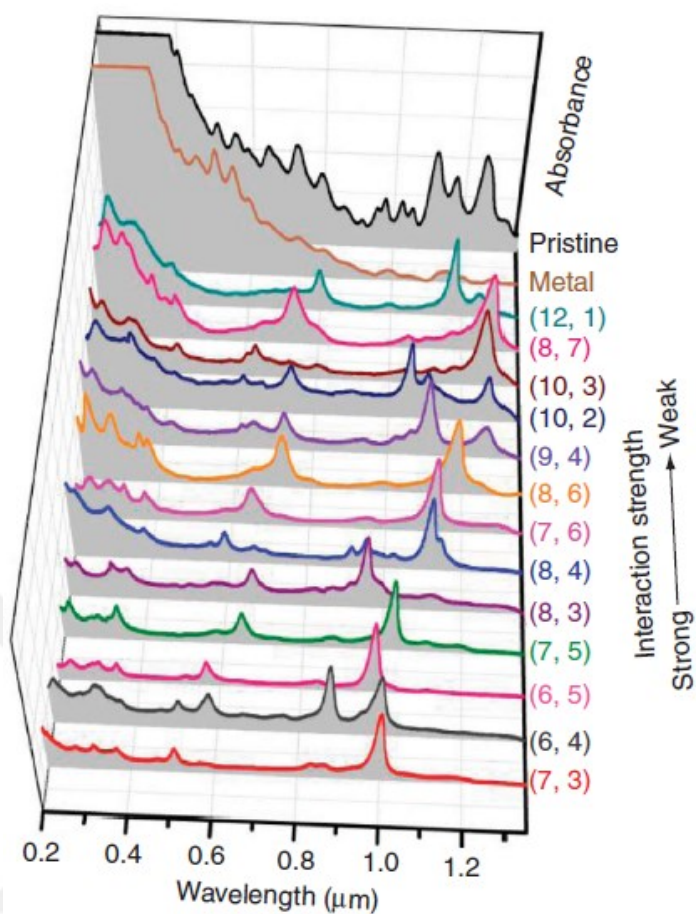
Figure 6.10 : Optical absorption spectra of chirality separation of SWCNTs using single-surfactant multicolumn gel chromatography[26].
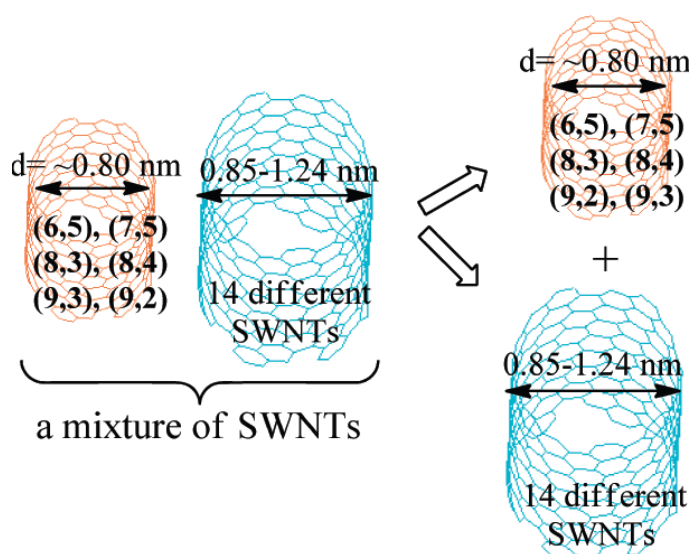
Figure 6.11 : Chirality of of small diameters (d = 0.75−0.84 nm) and large diameter (d = 0.85−1.24 nm) single-walled nanotubes (SWCNTs)[124].
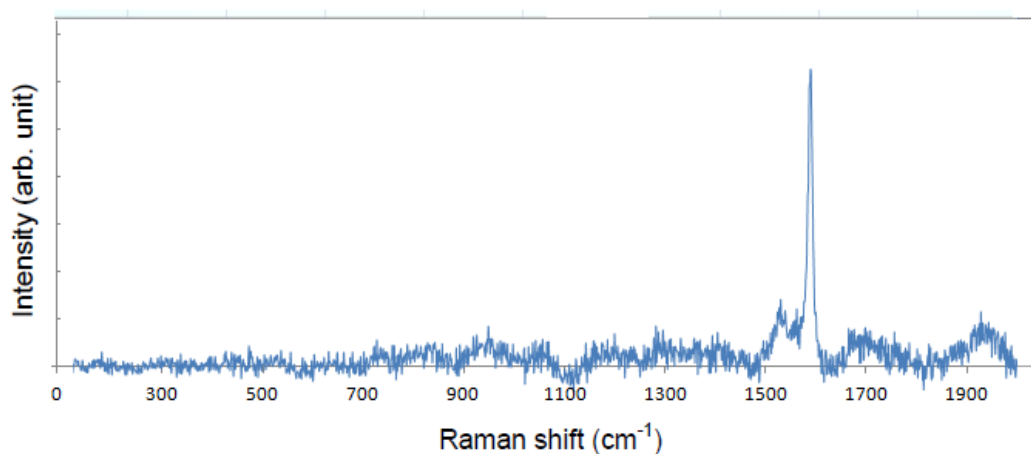
Figure 6.12 : Raman spectrum of solution of after applying 5% wt SDS in Sephacryl gel.

Figure 6.13 shows the absorption spectrum of small s-SWCNTs eluted by 1% wt SC whose difference with 5% wt SDS is the difference in s-SWCNTs chiralities
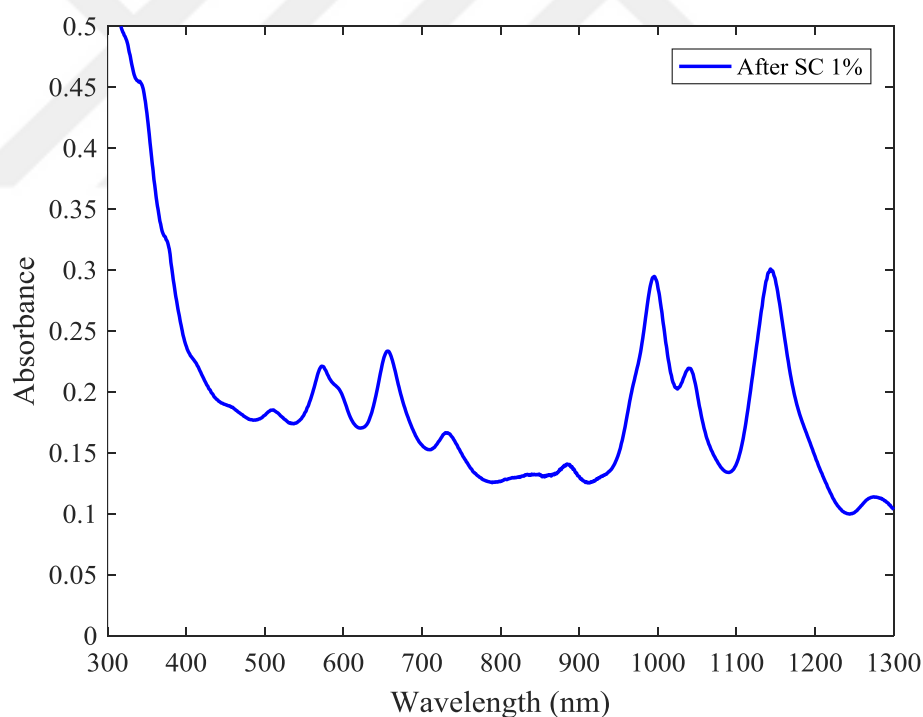
Figure 6.13 : Absorption spectrum after applying 1% wt SC in Sephacryl gel.

Figure 6.14 indicates absorption spectrum of unbundle solution after two times application of Sephacryl gel included column. This figure shows all s-SWCNTs are not adsorbed to the gel and, as a result, are not separated from pristine solution. By repeating the process of applying unbundle to gel there was not observed any change

in absorption spectrum. By comparing Figures 6.10 and 6.11 with 6.14, it can be resulted that s-SWCNTs remained in unbundle were large s-SWCNTs where the small ones were adsorbed to Sephacryl gel.
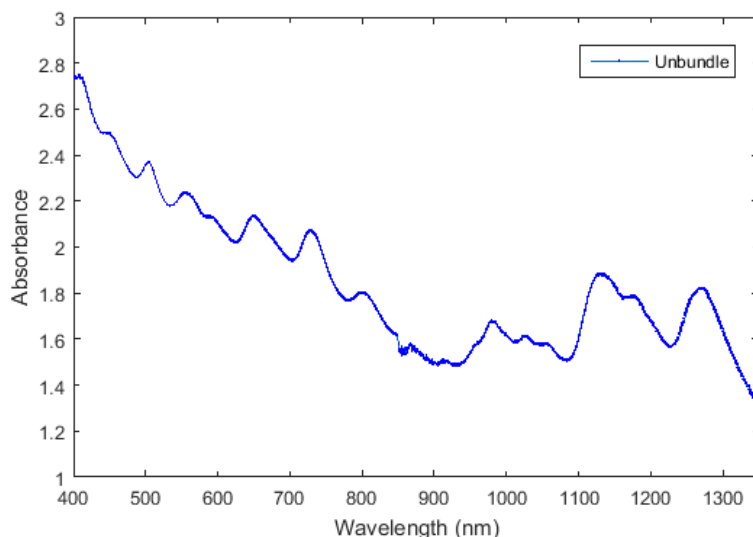
Figure 6.14 : UV-Vis-NIR spectrum of unbundle SWCNTs fter applying two times column of Sephacryl gel.

6.2.2 Adsorbing large diameter semiconducting SWCNTs to Agarose gel

Gel column was prepared by filling of 1.4 ml of Agorose gel. 1 % wt aqueous SDS solution was used to elute the metallic and unbound nanotubes until no nanotubes were detected in the eluent. To obtain metallic SWCNT, 1 % wt SDS (10ml) was used until no nanotubes were detected in the eluent. The s-SWCNTs adsorbed on the column were desorbed and collected by injection with 1% wt SC (10ml) was used to elute the s-SWCNTs adsorbed onto the gel at 1% wt SDS(10ml). To achieve the effective separation, we considered SWCNTs adsorbtion to the column with Agarose gel. When applying a gradient of the eluting surfactant to a column with semiconducting SWCNTs adsorbed to the gel, it was observed that the large diameter tubes elute from the column (with Sephacryl gel) before the smaller diameter tubes. Large diameter SWCNTs have more SDS on the surface due to the fact that the larger diameter allows for more conformational arrangements of the SDS on the SWCNT and finally is collected as unbundle solution. Under this conditions we missed large s-SWCNTs and have low yield separation processes, for solving this problem, we used Agarose gel that have a structure which large diameter SWCNTs will adsorb more strongly to the column and finally is separated as large s-SWCNTs.

Figure 6.13 indicates that separated large and small diameter s-SWCNTs with Agarose and Sephacryl gels that blue one is small semiconducting and green one is is large s-SWCNTs.
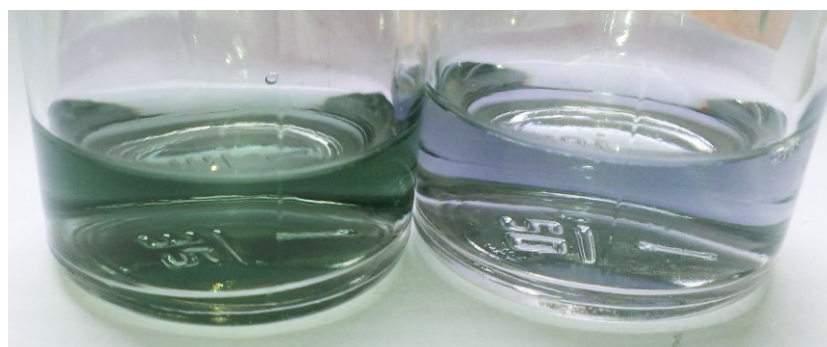
Figure 6.15 : Separated s-SWCNT with Sephacryl and Agarose gels (blue one is small s-SWCNTs and green one is large s-SWCNTs).

Figure 6.14 shows the absorption spectra of the sample after 1% wt SC for two consequtive column of Agarose gel. Large s-SWCNTs are adsorbed to Agarose gel and separated as expected. Gel chromatography process was repeated for increasing the efficiency by further adsorbing of large s-SWCNTs to the gel inside the column.
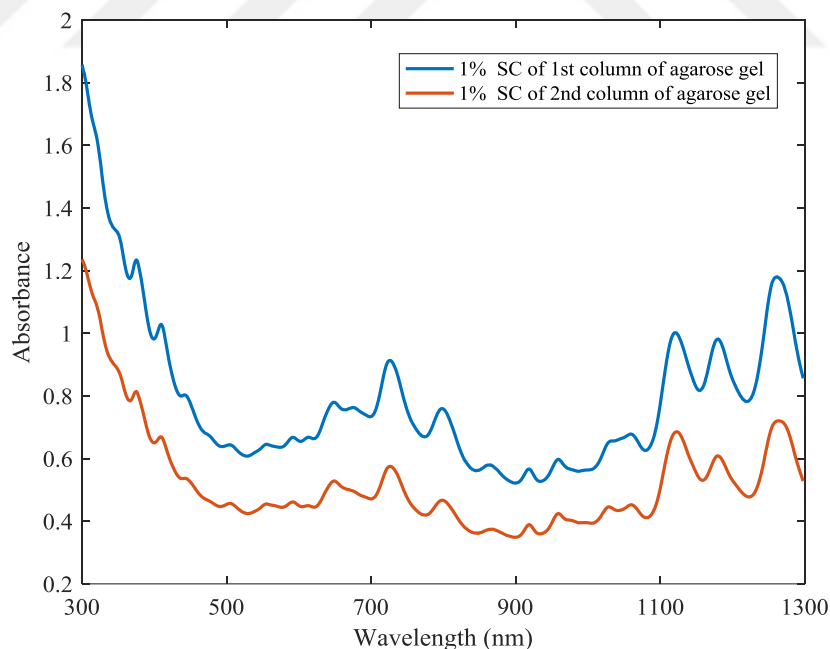
Figure 6.16 : Separated large diameter s-SWCNTs that applied in Agarose gel for two times after applying sample solution in two times of Sephacryl gel.

Figure 6.17 indicates unbundle sample after applying the first and second columns of Agarose gel. It can be seen that after the second column process all large s-SWCNTs

are separated from the pristine sample. According to experimental results, the optimum number of repetition is one (totally 2 times of operation) for each gel. This amount of process is fairly enough for obtaining the pure s-SWCNTs. Since, as can be seen from Figure, there is no corresponded component to s-SWCNTs visible in the spectrum within unbundle of the second column of Agarose gel.
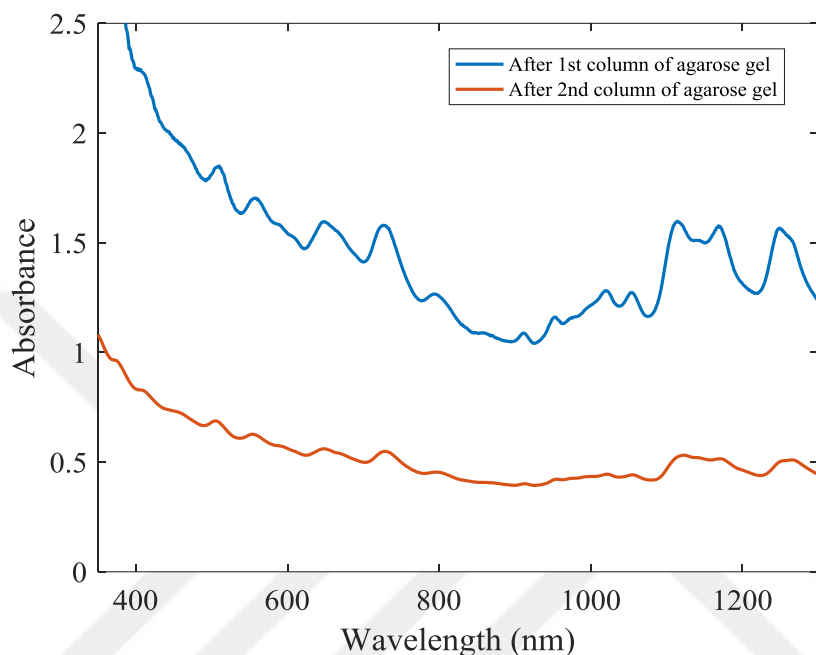
Figure 6.17 : Unbundle of after applying sample in two Agarose column.

6.2.3 Enrichment of m-SWCNTs

Metallic nanotubes exhibited the lowest interaction with the gels and so were finally collected as unbound nanotubes. The evolution of the surfactant structure on a nanotube sidewall is also proposed to change from random adsorption at low surfactant concentration, to hemispherical-micelle/micelle adsorption at intermediate concentration, and finally to micellar or aggregate encapsulation at higher concentrations. Metallic species possess greater surfactant coverage, which facilitates their rapid passage through the gel medium.

In order to find the micelle concentration of SDS we performed the experments with 0.3%, 0.5% and 1% wt SDS. As can be seen from Figure 6.18, any considerable difference between 0.5% and 1% wt SDS was not observed, therefore we chose 1% wt SDS as the experimental condition, however in the literature the 0.5% wt SDS is known as the best concentration.
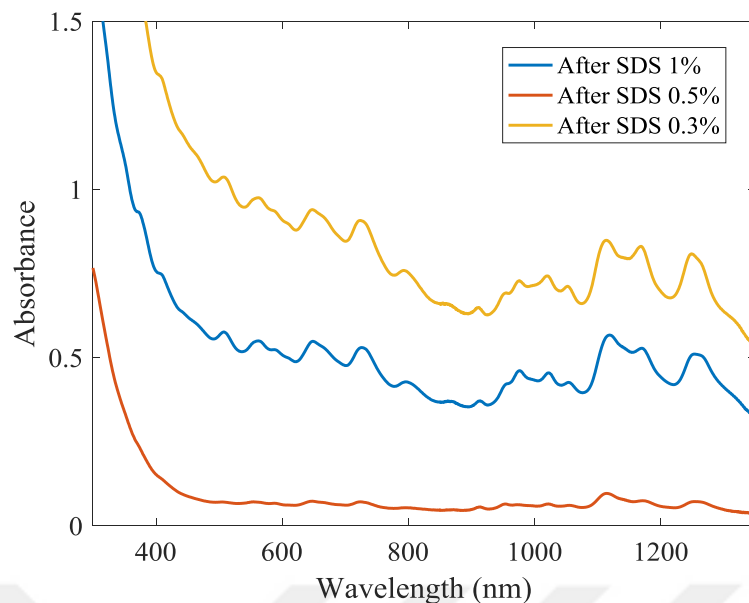
Figure 6.18 : The absorption spectra of solution after various SDS concentrations.

To obtain purer m-SWCNTs, after completing separation of m-SWCNTs with applied 1% wt SDS in Sephacryl gel, we applied this solution to second column for removing resedual s-SWCNTs. Figure 6.19 shows the optical absorption spectra of the m-SWCNTs after first column and applying it on second column. As can be seen after the second application to the column, s-SWCNTs adsorbed to gel and m-SWCNTs will pass the gel. As the final result we can obtain purer s-SWCNT and m-SWCNT the by this proposed method.
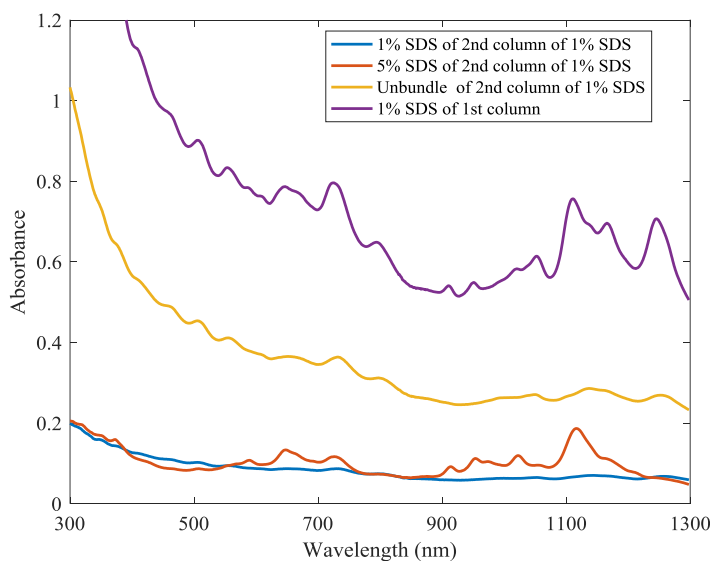
Figure 6.19 : Absorption spectra of enrichment m-SWCNTs with applying on 2nd column.

61

7. CONCLUSIONS AND RECOMMENDATIONS

In this study, gel chromatoghraphy method was utilized for separation of HiPco SWCNTs. The effects of gel matrix and SDS concentration were investigated on duration of separation processes. Besides, enrichment studies of the m-SWCNT and s-SWCNT species were performed using both Sephacryl and Agarose gels. Important findings of this study are as follows:

7.1 Concluding Remarks

1. In this thesis, the motivation was to propose an effective, low cost and low complexity with minimum number of required processes for separation of s-SWCNT and m-SWCNT from the raw SWCNT. Presented method is based on gel chromatography and provides very simpler and more reliable process with only four column repetition comparing with the literatures from the well-known research groups working in this area which require 40-60 column repetition for the same efficiency.

2. Both m-SWCNT and s-SWCNT separation were achieved containing several chiralities. To obtain m- SWCNT, 1 % wt SDS was used until no nanotubes were detected in the eluent. The s-SWCNTs adsorbed on the column were desorbed and collected by injection with a 5 %wt SDS until no absorbance was detected. Then1% wt SC was used to elude the s-SWCNTs adsorbed onto the gel at 5% wt SDS.

3. Related to the diameter and chirality distributions of nanotubes, m-SWCNTs were observed with a color gradient of brown and s-SWCNTs were observed with a color gradient of blue where stationary phase is Sephacryl 200 gel. However, s-SWCNTs were observed with a color gradient of green where stationary phase is Agarose gel.

4. The various m- SWCNT and s-SWCNT fractions demonstrated significant differences in their diameter distributions with high purity and high yield. The

separated SWCNTs were characterized with UV-vis -NIR and Raman spectroscopy.

5. Sonication duration is one of the most important parameters for preparation of homogeneous SWCNT solutions. Based on our experiments, the optimum sonication duration was found as120 minutes.

6. One of the most important factors in separation is the type of SWCNTs. Hipco SWCNT which used in this study, is the most appropriate type for this purpose.

7. As the loading amount of SWCNT dispersion is increased, the nanotubes exhibiting the strongest interaction with the gel eventually replace the other nanotubes and occupy all the adsorption sites.

8. Smaller diameter s-SWCNTs with higher affinity adsorb more strongly to the column with Sephacryl gel while large diameter SWCNTs adsorb weakly to the column with this gel.

9. Large diameter s-SWCNTs with higher affinity adsorb more strongly to the column with Agarose gel.

10. The energy bandgap of s-SWCNT is inversely proportional to the nanotube diameter. Accordingly, in absorption spectra, peaks in higher wavelength (>1200 nm) indicate large diameter s-SWCNTs, while peaks in lower wavelength (<1200 nm) indicate small diameter s-SWCNTs. Thus, correspond to interactions between nanotubes and gel medium, small diameter s-SWCNTs were obtained using with Sephacryl 200 gel and large diameter s-SWCNTs were obtained using with Agarose gel as stationary phase.

11. High yield of separation is obtained by using Sephacryl and Agarose gels consequently. The optimum number of repeat for each gel step was found to be two times.

7.2 Recommendations

The research performed in this thesis focused on separation of SWCNTs by electronic structure using gel chromatography. In recent years, selective enrichment and separation of SWCNTs play a vital role in the realization of the potential application of m-SWCNTs and s-SWCNTs having several advantageous. Therefore, the

separation with the high efficiency of both m-SWCNTs and s-SWCNTs is of great importance. Separation of different types of SWCNTs, however, remains one of the fundamental and challenging issues in nano science. In this aspect, sorting m-SWCNTs and s-SWCNTs using gel chromatography is one of the very promising SWCNT separation method in terms of especially simplicity of application. Consequently, we separated nearly all of the small and large m-SWCNTs and s-SWCNTs that passed through the final column as unbundle solution. The most importance of this Thesis is using Sephacryl and Agarose gels respectively, usage one of these gels leads to low separation yield, but we reached to high yield with usage both of these gels. By only four repetitions (two time with each gel), this method is becoming very simple and low cost that can be used for large-scale with higher throughput from raw SWCNTs separation comparing with previously reported methods in literature.

Future studies including the gel chromatography discussed in this thesis will require enrichment of separation processes such as optimization of dispersion methodology for increasing of SWCNT-surfactant interactions or utilization of distinct dextran based gels as stationary phase for providing selective adsorption of m-SWCNTs and s-SWCNTs.

REFERENCES

[1] **Pileni, M.P. (**2002). Nanostructured materials, Selected synthesis methods, properties and applications, edited by Knauth, P., Schoonman, J., Kluwer Academic Publishers, pp 122.

[2] **Kroto, H. W., Heath, J. R., O'Brien, S. C., Curl, R. F., and Smalley, R. E.** (1985). C60Buckminsterfullerene, Nature, Vol. 318, p. 162.

[3] **Iijima, S.** (1991). Helical microtubules of graphitic carbon, Nature, Vol. 354, pp. 56–58.

[4] **Iijima, S. and Ichihashi, T.** (1993). Single-shell carbon nanotubes of 1nm diameter. Nature, Vol 363, pp. 603–615.

[5] **Bachilo, S. M., Balzano, L., Herrera, J. E., Pompeo, F., Resasco, D. E., Weisman, R. B.** (2003). Narrow (n, m)-distribution of single-walled carbon nanotubes grown using a solid supported catalyst. Journal o f the American Chemical Society .125, (37), 11186-11187.

[6] **Chattopadhyay, D., Galeska, I., Papadimitrakopoulos, F.** (2003). A route for bulk separation of semiconducting from metallic single-wall carbon nanotubes. Journal o f the American Chemical Society. 125, (11), 3370-3375.

[7] **Zheng, Ming, et al.** (2003). Structure-based carbon nanotube sorting by sequence-dependent DNA assembly. Science. 302, (5650), 1545-1548.

[8] **Chen, Zihong; et al. (**2003)**.** Bulk separative enrichment in metallic or semiconducting single-walled carbon nanotubes. Nano Letters. 3, (9), 1245-1249.

[9] **Krupke, Ralph, et al. (**2003). Separation of metallic from semiconducting single-walled carbon nanotubes Science. 301, (5631), 344-347.

[10] **Maeda, Yutaka, et al.** (2006). Dispersion and separation of small-diameter single-walled carbon nanotubes." *Journal of the American Chemical Society* 128.37. 12239-12242.

[11] **Samsonidze, Ge G., et al.** (2004). Quantitative evaluation of the octadecylamine-assisted bulk separation of semiconducting and metallic single-wall carbon nanotubes by resonance Raman spectroscopy. Applied Physics Letters. 85, (6), 1006-1008.

[12] **Liu, Jie, et al.** (1998). Fullerene pipes. Science (Washington, D. C.).280, (5367), 1253-1256.

[13] **Ramesh, S.; Ericson, L. M.; Davis, V. A.; Saini, R. K.; Kittrell, C.; Pasquali, M.; Billups, W. E.; Adams, W. W.; Hauge, R. H.; Smalley, R. E.** (2004). Dissolution of pristine single walled carbon nanotubes in superacids by direct protonation. Journal o f Physical Chemistry B. 108, (26), 8794-8798.

[14] **Souza Filho, A. G.; Jorio, A.; Samsonidze, G. G.; Dresselhaus, G.; Saito, R.; Dresselhaus, M. S.** (2003). Dissolution of pristine single walled carbon nanotubes in superacids by direct protonation. Nanotechnology. 14, (10), 1130-1139.

[15] **Strano, Micheal S. et al, (**2003). Reversible, band-gap-selective protonation of single-walled carbon nanotubes in solution**.** Journal o f Physical Chemistry B 107, (29), 6979-6985.

[16] **Kukovecz, A.; Pichler, T.; Pfeiffer, R.; Kuzmany, H. (**2002). Chemical Communications (Cambridge, United Kingdom) . (16), 1730-1731.

[17] **Corio, P.; Jorio, A.; Demir, N.; Dresselhaus, M. S. (**2004). Spectro-electrochemical studies of single wall carbon nanotubes films. Chemical Physics Letters 392, (4-6), 396-402.

[18] **Luo, Z.; Li, R.; Kim, S. N.; Papadimitrakopoulos, F.** (2004). Physical Review B: Condensed Matter and Materials Physics. 70, (24), 245429/1-245429/8.

[19] **Brar, V. W., et al. (**2005). Resonance Raman spectroscopy characterization of single-wall carbon nanotube separation by their metallicity and diameter."*Journal of nanoscience and nanotechnology* Journal o f Nanoscience and Nanotechnology. 5, (2), 209-228.

[20] **Ebbesen, T. W.; Hiura, H.; Fujita, J.; Ochiai, Y.; Matsui, S.; Tanigaki, K. (**1993). Patterns in the bulk growth of carbon nanotubes. Chemical Physics Letters. 209, (1-2), 83-90.

[21] **Krupke, R.; Hennrich, F.; Löhneysen, H. V.; Kappes, M. M.** (2003). Separation of Metallic from Semiconducting Single- Walled Carbon Nanotubes. Science, 301, 344–347.

[22] **Zheng, M.; Jagota, A.; Strano, M. S.; Santos, A. P.; Barone, P.; Chou, S. G.; Diner, B. A.; Dresselhaus, M. S.; McLean, R. S.; Onoa, G. B.; et al. (**2003). Structure-Based Carbon Nanotube Sorting by Sequence-Dependent DNA Assembly. Science. 302, 1545–1548.

[23] **Park, S.; Lee, H. W.; Wang, H.; Selvarasah, S.; Dokmeci, M. R.; Park, Y. J.; Cha, S. N.; Kim, J. M.; Bao, Z. (**2012). Highly Effective Separation of Semiconducting Carbon Nanotubes Verified via Short-Channel Devices Fabricated Using Dip-Pen Nanolithography. ACS Nano 6, 2487–2496.

[24] **Blum, C.; Stürzl, N.; Hennrich, F.; Lebedkin, S.; Heeg, S.; Dumlich, H.; Reich, S.; Kappes, M. M.** (2011). Selective Bundling of Zigzag Single-Walled Carbon Nanotubes. ACS Nano. 5, 2847–2854.

[25] **Miyata, Y.; Shiozawa, K.; Asada, Y.; Ohno, Y.; Kitaura, R.; Mizutani, T.; Shinohara, H. (**2011). Length-Sorted Semiconducting Carbon Nanotubes for High-Mobility Thin Film Transistors. Nano Res. 4, 963–970.

[26] **Liu, H.; Nishide, D.; Tanaka, T.; Kataura, H. (**2011). Large-Scale Single-Chirality Separation of Single-Wall Carbon Nanotubes by Simple Gel Chromatography. Nat. Commun. 2, 309–8.

[27] **S. Ghosh, S. M. Bachilo, and R. B.** (2010). Weisman, Nature Nanotechnol. 5, 443

[28] **Ju SY, Utz M, Papadimitrakopoulos F. (**2009). Enrichment mechanism of semiconducting single-walled carbon nanotubes by surfactant amines. J Am Chem Soc; 131:6775–84.

[29] **Pierson, H. O.** (1993). *Handbook of carbon, graphite, diamond and fullerenes*. Noyes Publications.

[30] **Popov, V. N.** (2004). Carbon Nanotubes: Properties and Applications. *Mater. Sci. Eng. R-Reports*, *43*, 61–102.

[31] **Harris, P. J. F.** (1999). *Carbon Nanotubes and Related Structures*. Cambridge University Press.

[32] **Meyyappan, M.** (2004). *Carbon Nanotubes: Science and Applications*. CRC Press.

[33] **Govindaraj, A.** (2005). *Nanotubes and Nanowires*. RSC Publications.

[34] **Dresselhaus, M. S., Dresselhaus, G., Avouris, P.** (2001). Eds., *Carbon Nanotubes*, *80*. Berlin, Heidelberg: Springer Berlin Heidelberg.

[35] **Journet, C. M., W. K.; Bernier, P.; Loiseau, A.; de la Chapelle, M. L.; Lefrant, S.; Deniard, P.; Lee, R.; Fischer, J. E.** (1997) Nature, 388, 756-58.

[36] **Bronikowski, M. J.; Willis, P. A.; Colbert, D. T.; Smith, K. A.; Smalley, R. E. (**2001). Journal of Vacuum Science & Technology A: Vacuum, Surfaces, and Films, 19, (4),1800.

[37] **Bachilo, S. M. B., L.; Herrera, J. E.; Pompeo, F.; Resasco, D. E.; Weisman, R. B. J. Am.** (2003). Chem. Soc. 125, 11186-87.

[38] **Weisman, R. B.; Bachilo, S. M.** (2003). Nano letters, 3, (9), 1235-1238.

[39] **White, C. T.; W., M. J. J. (**2005) Phys. Chem. B, 109, 52-65.

[40] **Bachilo, S. M.; Strano, M. S.; Kittrell, C.; Hauge, R. H.; Smalley, R. E.; Weisman, R. B.** (2002). Science, 298, 2361-2366.

[41] **Javey, A.** (2008). ACS nano, 2, (7), 1329-35.

[42] **Jorio, A.; Dresselhaus, G.; dresselhaus, M. S.** (2008). Carbon Nanotubes-advanced topics in the sythesis, structure, properties and applications. Springer: Berlin.

[43] **Weisman, R. B.; Bachilo, S. M.** (2003). Nano letters, 3, (9), 1235-1238.

[42] **Saito, R.; Dresselhaus, G.; Dresselhaus, M. S.** (1998). Physical Properties of Carbon Nanotubes; Imperial College Press: London.

[43] **Bachilo, S. M.; Strano, M. S.; Kittrell, C; Hauge, R. H.; Smalley, R. E.; Weisman, R. B. (**2002). Structure-Assigned Optical Spectra of Single-Walled Carbon Nanotubes. Science,298, 2361-2366.

[44] **Dresselhaus, M.S., Dresselhaus, G., and Avouris, P.** (2001). Carbon nanotubes: Synthesis, structure, properties and applications, Springer, London.

[45] **Chico, L., Crespi, V. H., Benedict, L. X., Louie, S. G., Cohen, M. L.** (1996). Pure carbon nanoscale devices: Nanotube heterojunctions, Physical Review Letters, Vol. 76, pp. 971–974.

[46] **Saito, R., Fujita M., Dresselhaus, G., Dresselhaus, M. S.** (1992). Electronic structure of chiral graphene tubules, Applied Physics Letters, Vol. 60, pp.2204–2206. 91.

[47] **Mintmire, J.W., Dunlap, B. I., White, C. T.** (1992). Are fullerene tubules metallic? Physical Review Letters, Vol. 68, pp. 631−634.

[48] **Vodenitcharova, T., and Zhang, L.C.** (2003). Effective wall thickness of a singlewalled carbon nanotube, Physical Review B, Vol. 68, 165401

[49] **Hone, J**. (2004) Carbon nanotubes: Thermal properties. Dekker Encyclopedia of Nanoscience and Nanotechnology, DOI: 10.1081/EENN 120009128, Columbia University, NewYork.

[50] **AnonymousAudacious & Outrageous: Space Elevators.** http://spacescience.com/headlines/y2000/ast07sep_1.htm?list2007).

[51] **Nalwa, H. S.** (2000). In Handbook of nanostructured materials and nanotechnology; Academic Press: San Diego.

[52] **Ajayan, P. M.; Stephan, O.; Colliex, C.; Trauth, D.** (1994). Science, 265, 1212-1214.

[53] **Hartschuh, A.; Pedrosa, H. N.; Peterson, J.; Huang, L.; Anger, P.; Qian, H.; Meixner, A. J.; Steiner, M.; Novotny, L.; Krauss, T. D. (**2005). Chem.Phys. Chem. 6, 577-582.

[54] **Song, C.; Pehrsson, P. E.; Zhao, W. J.** (2005). Recoverable solution reaction of HiPco carbon nanotubes with hydrogen peroxide. Phy.s Chem. B, 109, 21634-21639.

[55] **Song, C.; Pehrsson, P. E.; Zhao, W. J.** (2006). Optical enzymatic detection of glucose based on hydrogen peroxide-sensitive HiPco carbon nanotubes. Mater. Res. 21, 2817-2823.

[56] **Kelley, K; Pehrsson, P. E.; Ericson, L. M.; Zhao, W. J.** (2005). Optical pH response of DNA wrapped HiPco carbon nanotubes. Nanosci. Nanotechnol. 5, 1029-1032.

[57] **Daenen, M.; de Fouw, R. D.; Hamers, B.; Janssen, P. G. A.; Schouteden, K.; Veld, M. M. A. J. (**2003). Review of Current Carbon nanotube Technologies;

[58] **Yu, Z.; Brus, L. E. J.** (2001). (n, m) structural assignments and chirality dependence in single-wall carbon nanotube Raman scattering. Phys. Chem. B, 105, 6831-6837.

[59] **Ruoff, Rodney S., and Donald C. Lorents.** (1995). Mechanical and thermal properties of carbon nanotubes. carbon 33.7. 925-930. APA.

[60] **Hone, J., Whitney, M., Zettl, A.** (1999). Thremal conductivity of single walled carbon nanotubes, Synthetic metals, Vol. 103, pp. 24982499.

[61] **Cao, A., Xu, C., Liang, J., Wu, D., Wei., B.** (2001). X ray diffraction characterization on the alignment degree of carbon nanotubes, Chemical Physics Letters, Vol. 344, pp. 1317.

[62] **Berber, S., Kwon, Y. K., Tomanek, D.** (2000). Unusually high thermal conductivity of carbon nanotubes, Physics Review Letter, Vol. 84, pp. 46134616.

[63] **O'Connel, M.J.** (2006). Carbon nanotubes: Properties and Applications, Taylor & Francis., Florida.

[64] **Popov, V. N.** (2004). Carbon nanotubes: properties and applications. Materials Science and Engineering R, 43, 61102

[65] **Wang, M., Zhao, X. L., Ohkohchi, M., Ando, Y.** (1996). Carbon nanotubes grown on the surface of cathode deposit by arc discharge, Fullerene Science and Technology, Vol. 4, pp. 10271039.

[66] **T. W. Ebbesen.** (1994). Carbon nanotubesreview. Annual Review of Materials Science, Vol. 24, pp. 235264.

[67] **Burchell, T. D.** (1999). Carbon materials for advanced technologies, Pergamon, Oak Ridge

[68] **Journet, C., Maser, W. K., Bernier, P., Loiseau, A., dela Chapelle, M. L., Lefrant, S., Deniard, P., Lee, R., and Fischer, J. E.** (1997) Largescale production of singlewalled carbon nanotubes by the electricarc technique. Nature, Vol. 388, pp. 756–758.

[69] **Endo, M., Takeuchi, K., Igarashi, S., Kobori, K., Shiraishi, M., and Kroto, H.W.** (1993). The production and structure of pyrolytic carbon nanotubes (PCNTs). Journal of the Physics and Chemistry of Solids Vol. 54, pp. 1841–1848.

[70] **O'Connel, M.J.** (2006). Carbon nanotubes: Properties and Applications, Taylor & Francis., Florida.

[71] **Oncel, Ç., and Yurum, Y.** (2006) Carbon nanotube synthesis via catalytic CVD method: A review on the effect of reaction parameters. Fullerenes, nanotubes and carbon nanostructures, Vol. 14, pp. 1737

[72] **Arnold, M. S.; Stupp, S. I.; Hersam, M. C. (**2005). Enrichment of Single-Walled Carbon Nanotubes by Diameter in Density Gradients. Nano Lett. 5, 713-718.

[73] **Zhao, Pei, et al**. (2011). Tunable separation of single-walled carbon nanotubes by dual-surfactant density gradient ultracentrifugation." Nano Research 4.7. 623-634.

[74] **Wang, H.; Zhou, W.; Ho, D. L.; Winey, K. L.; Fischer, J. E.; Glinka, C. J.; Hobbie, E. K.** (2004). Dispersing Single-Walled Carbon Nanotubes with Surfactants: A Small Angle Neutron Scattering Study. Nano Lett. 4, 1789-1793.

[75] **Arnold, M. S.; Green, A. A.; Hulvat, J. F.; Stupp, S. I.; Hersam, M. C.** Nature Nanotechnology, 2006, 1, 60-65.

[76] **Ghosh, S.; Bachilo, S. M.; Wesiman, R. B. (**2010). Nature Nanotechnology, 5, 443- 450.

[77] **Tanaka, T.; Jin, H.; Miyata, Y.; Fujii, S.; Suga, H.; Naitoh, Y.; Minari, T.; Miyadera, T.; Tsukagoshi, K.; Kataura, H.** (2009). Nano Lett. 9 (4), 1497−1500.

[78] **Tanaka, T.; Jin, H.; Miyata, Y.; Kataura, H.** (2008). Appl. Phys. Express, 1 (11), 1140011−1140013.

[79] **Kong, Jing, and Hongjie Dai. (**2011). Full and modulated chemical gating of individual carbon nanotubes by organic amine compounds. The Journal of Physical Chemistry B 105.15. 2890-2893.

[80] **Maeda, Y.; Kanda, M.; Hashimoto, M.; Hasegawa, T.; Kimura, S. I.; Lian, Y.; Wakahara, T.; Akasaka, T.; Kazaoui, S.; Minami, N. J. Am.** (2006). Chem. Soc. 128 (37), 12239−12242

[81] **Sara Mesgari, Yin Fun Poon, Liang Yu Yan, Yuan Chen, Leslie S. Loo, Ya Xuan Thong, and Mary B. Chan-Park.** (2012). Acs, 116, 10266−10273

[82] **Blanch, Adam J., Jamie S. Quinton, and Joe G. Shapter.** (2013). The role of sodium dodecyl sulfate concentration in the separation of carbon nanotubes using gel chromatography. *Carbon* 60, 471-480.

[83] **Huang X, Mclean R. S. and Zheng M. (**2005). High-resolution length sorting and purification of DNA-wrapped carbon nanotubes by sizeexclusion chromatography Anal. Chem. 77 6225–8

[84] **Lee W, Cho Y J, Choi H R, Park H J, Chang T, ParkMand Lee H.** (2012) Elution behavior of shortened multiwalled carbon nanotubes in size exclusion chromatography J. Sep. Sci. 35 3250–6

[85] **Asada Y, Sugai T, Kitaura R. and Shinohara H. (**2009) Chromatographic length separation and photoluminescence study on DNAwrapped single-wall and double-wall carbon nanotubes J. Nanomater. 2009 36

[86] **Liu H, Nishide D, Tanaka T and Kataura H**. (2011). Large-scale single-chirality separation of single-wall carbon nanotubes by simple gel chromatography Nat. Commun. 2 309

[87] **Moshammer, K. , Hennrich , F . & Kappes, M. M.** (2009). Selective suspension in aqueous sodium dodecyl sulfate according to electronic structure type allows simple separation of metallic from semiconducting single-walled carbon nanotubes. Nano Res. 2, 599 – 606

[88] **Liu, H.; Nishide, D.; Kataura, H**. (2011). Nature Communications, 2, 309.

[89] **Thendie, Boanerges, et al.** (2013). Rapid Single-Stage Separation of Micrometer-Long and High-Purity Semiconducting Carbon Nanotubes by Gel Filtration. *Applied Physics Express* 6.6 065101.

[90] **Liu, H.; Tanaka, T.; Urabe, Y.; Kataura, H.** (2013). High-Efficiency Single-Chirality Separation of Carbon Nanotubes Using Temperature-Controlled Gel Chromatography. Nano Lett. 13, 1996−2003.

[91] **Hirano, A.; Tanaka, T.; Urabe, Y.; Kataura, H.** (2013). pH- and Solute-Dependent Adsorption of Single-Wall Carbon Nanotubes onto Hydrogels: Mechanistic Insights into the Metal/Semiconductor Separation. ACS Nano, 7, 10285−10295.

[92] **Flavel, B. S.; Moore, K. E.; Pfohl, M.; Kappes, M. M.; Hennrich, F.** (2014). Separation of Single-Walled Carbon Nanotubes with a Gel Permeation Chromatography System. ACS Nano, 8, 1817−1826.

[93] **Jain, Rishabh M., et al.** (2015). Competitive Binding in Mixed Surfactant Systems for Single-Walled Carbon Nanotube Separation. The Journal of Physical Chemistry C 119.39 22737-22745. APA

[94] **Flavel, Benjamin S., et al.** (2013). Separation of single-walled carbon nanotubes by 1-dodecanol-mediated size-exclusion chromatography. ACS nano. 7.4 3557-3564.

[95] **Tulevski, George S., Aaron D. Franklin, and Ali Afzali.** (2013). High purity isolation and quantification of semiconducting carbon nanotubes via column chromatography." ACS nano. 7.4 2971-2976.

[96] **Tanaka, Takeshi, et al.** (2015) Simultaneous chirality and enantiomer separation of metallic single-wall carbon nanotubes by gel column chromatography."Analytical chemistry. 87.18 9467-9472

[97] **Maeda, Yutaka, et al**. (2005). "Large-scale separation of metallic and semiconducting single-walled carbon nanotubes." *Journal of the American Chemical Society.* 127.29 10287-10290.

[98] **Maeda, Yutaka, et al.** (2010). Separation of metallic single-walled carbon nanotubes using various amines." *physica status solidi (b)* 247.11-12. 2641-2644.

[99] **Maeda, Yutaka, et al.** (2012). Interaction of single-walled carbon nanotubes with amine." *Nano* 7.01. 1130001.

[100] **C.W. Ooi, B.T. Tey, S.L. Hii, S. Mazlina, M. Kamal, J.C.W. Lan, A. Ariff, T.C. Ling.** (2009). Purification of lipase derived from Burkholderia pseudomallei with alcohol/salt-based aqueous two-phase systems, Process Biochem. 44 1083– 1087.

[101] **L. Bulgariu, D. Bulgariu,** (2008). Extraction of metal ions in aqueous polyethylene glycol-inorganic salt two-phase systems in the presence of inorganic extractants: correlation between extraction behaviour and stability constants of extracted species, J. Chromatogr. A 1196. 117– 124.

[102] **M. Pereira, Y.T. Wu, A. Venancio, J. Teixeira.** (2003). Aqueous two-phase extraction using thermo separating polymer: a new system for the separation of endopolygalacturonase, Biochem. Eng. J. 15. 131–138.

[103] **P.Y. Bi, D.Q. Li, H.R. Dong,** (2009). A novel technique for the separation and concentration of penicillin G from fermentation broth: aqueous two-phase flotation, Sep. Purif. Technol. 69. 205–209.

[104] **L. Stobinski, E. Polaczek, K. Rebilas, J. Mazurkiewicz, R. Wrzalik, H.M. Lin, P. Tomasik,** (2008). Dextran complexes with single-walled carbon nanotubes, Polimery 53. 571–575.

[105] **C. Ozdemir, A. Guner,** (2007). Solubility profiles of poly(ethylene glycol)/solvent systems, I: qualitative comparison of solubility parameter approaches, Eur. Polym. J. 43 3068–3093.

[106] **T. Hasan, V. Scardaci, P.H. Tan, A.G. Rozhin, W.I. Milne, A.C. Ferrari,** Stabilization and ''Debundling'' of single-wall carbon nanotube dispersions.

[107] **D. Chattopadhyay, L. Galeska, F. Papadimitrakopoulos,** (2003). A route for bulk separation of semiconducting from metallic single-wall carbon nanotubes, J. Am. Chem. Soc. 125. 3370–3375.

[108] **Tang, Malcolm SY, et al.** (2014). Separation of single-walled carbon nanotubes using aqueous two-phase system." *Separation and Purification Technology* 125. 136-141.

[109] **Chen, F.; Wang, B.; Chen.** (2007). Y.; Li, L. Toward the extraction of single species of single-walled carbon nanotubes using fluorene-based polymers Nano Lett. 7, 3013-3017.

[110] **Hwang, J.; Nish, A.; Doig, J.; Douven, S.; Chen, C.; Chen, L.; Nicholas, R. J. J.** (2008). Polymer structure and solvent effects on the selective dispersion of single-walled carbon nanotubes. Am. Chem. Soc. 130, 3543-3553.

[111] **Nish, A.; Hwang, J.; Doig, J.; Nicholas, R. J.** (2007). Highly selective dispersion of single-walled carbon nanotubes using aromatic polymers. Nature Nanotechnology, 2, 640-646.

[112] **Chen, Yusheng, et al.** (2012). Achieving diameter-selective separation of single-walled carbon nanotubes by using polymer conformation-confined helical cavity." *ACS Macro Letters* 1.6. 701-705.

[113] **Carlson, Lisa J., and Todd D. Krauss.** (2008). Photophysics of individual single-walled carbon nanotubes. Accounts of chemical research 41.2. 235-243.

[114] **White, Carter T., and John W. Mintmire.** (2005). Fundamental properties of single-wall carbon nanotubes. The Journal of Physical Chemistry B 109.1 52-65.

[115**] Shim, M.; Kam, N. W. S.; Chen, R. J.; Li, Y.; Dai, H.** (2002). Functionalization of carbon nanotubes for biocompatibility and biomolecular recognition Nano Lett 2, 285-288.

[116] **Chen, Z. H.; Du, X.; Du, M. H.; Rancken, C. D.; Cheng, H. P.; Rinzler, A. G.** (2003). Bulk Separative Enrichment in Metallic or Semiconducting Single-Walled Carbon Nanotubes. Nano Lett. J, 1245-1249.

[117] **Itkis, M. E.; Perea, D. E.; Niyogi, S.; Rickard, S. M.; Hamon, M. A.; Zhao, B.; Haddon, R. C.** (2003). Purity Evaluation of As-Prepared Single-Walled Carbon Nanotube Soot by Use of Solution-Phase Near-IR Spectroscopy. Nano Lett. 3, 309- 314.

[118**] Strano, Michael S., et al.** (2003). Electronic structure control of single-walled carbon nanotube functionalization. *Science* 301.5639. 1519-1522.

[119] **Tu, Xiaomin, et al.** (2009). DNA sequence motifs for structure-specific recognition and separation of carbon nanotubes. *Nature* 460.7252 250-253.

[120] **Bachilo, S. M.; Strano, M. S.; Kittrell, C.; Hauge, R. H.; Smalley, R. E.; Weisman, R. B.** 2002. Science, 298, 2361-2366.

[121] **Ghosh, Saunab, Sergei M. Bachilo, and R. Bruce Weisman.** (2010). Advanced sorting of single-walled carbon nanotubes by nonlinear density-gradient ultracentrifugation. *Nature nanotechnology* 5.6. 443-450.

[122] **Rao, Apparao M., et al.** (1997). Diameter-selective Raman scattering from vibrational modes in carbon nanotubes. *Science* 275.5297 187-191.

[123] **Dr. Mildred Dresselhaus.** (2005). The presentation of carbon nanotube, MIT, NT05 Tutorial.

[124] **Chen, Yusheng, et al.** (2012) "Achieving diameter-selective separation of single-walled carbon nanotubes by using polymer conformation-confined helical cavity." *ACS Macro Letters* 1.6 701-705.

CURRICULUM VITAE
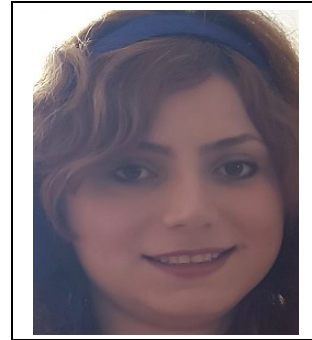
Name Surname: Fereshteh ORDOKHANI

Place and Date of Birth: Iran-24.06.85

E-Mail: f.ordokhani@gmail.com

EDUCATION:

B.Sc.: Solid-state physics- University of Tabriz/Iran